

## **NOTE TO USERS**

**This reproduction is the best copy available.**

UMI<sup>®</sup>



**INFLUENCE OF DISSOLVED OXYGEN ON THE  
PHYSICOCHEMICAL PROPERTIES AND  
MIGRATION BEHAVIOR OF SELECTED  
BACTERIAL PATHOGENS**

*by*

*Felipe Castro A.*

Department of Chemical Engineering  
McGill University, Montréal

October 2008

A THESIS SUBMITTED TO THE FACULTY OF GRADUATE STUDIES  
IN PARTIAL FULFILLMENT OF THE REQUIREMENTS FOR THE DEGREE OF  
MASTER OF ENGINEERING

Copyright © 2008 by Felipe Castro A.



Library and Archives  
Canada

Published Heritage  
Branch

395 Wellington Street  
Ottawa ON K1A 0N4  
Canada

Bibliothèque et  
Archives Canada

Direction du  
Patrimoine de l'édition

395, rue Wellington  
Ottawa ON K1A 0N4  
Canada

*Your file* *Votre référence*  
ISBN: 978-0-494-66948-8  
*Our file* *Notre référence*  
ISBN: 978-0-494-66948-8

**NOTICE:**

The author has granted a non-exclusive license allowing Library and Archives Canada to reproduce, publish, archive, preserve, conserve, communicate to the public by telecommunication or on the Internet, loan, distribute and sell theses worldwide, for commercial or non-commercial purposes, in microform, paper, electronic and/or any other formats.

The author retains copyright ownership and moral rights in this thesis. Neither the thesis nor substantial extracts from it may be printed or otherwise reproduced without the author's permission.

---

In compliance with the Canadian Privacy Act some supporting forms may have been removed from this thesis.

While these forms may be included in the document page count, their removal does not represent any loss of content from the thesis.

**AVIS:**

L'auteur a accordé une licence non exclusive permettant à la Bibliothèque et Archives Canada de reproduire, publier, archiver, sauvegarder, conserver, transmettre au public par télécommunication ou par l'Internet, prêter, distribuer et vendre des thèses partout dans le monde, à des fins commerciales ou autres, sur support microforme, papier, électronique et/ou autres formats.

L'auteur conserve la propriété du droit d'auteur et des droits moraux qui protègent cette thèse. Ni la thèse ni des extraits substantiels de celle-ci ne doivent être imprimés ou autrement reproduits sans son autorisation.

---

Conformément à la loi canadienne sur la protection de la vie privée, quelques formulaires secondaires ont été enlevés de cette thèse.

Bien que ces formulaires aient inclus dans la pagination, il n'y aura aucun contenu manquant.

  
**Canada**

## ABSTRACT

Protection of potable water supplies demands a better understanding of the factors controlling migration of disease causing bacteria in subsurface environments. In this study, the migration behaviour of the waterborne pathogenic microorganisms *Escherichia coli* O157:H7 and *Yersinia enterocolitica* was investigated in water saturated granular systems. Both facultative bacteria were grown under aerobic and anaerobic conditions and further acclimatized to a microaerophilic or fully aerated environment for 21 h. Experiments were conducted using laboratory-scale packed columns over controlled extreme dissolved oxygen (DO) concentrations. The observed differences in the transport potential of these pathogens were found to depend strongly on the antecedent growth conditions under the tested environmental settings as well with the environmental DO in certain conditions. Further microbial characterization using cell titrations and FTIR spectroscopy gave a greater insight on the source of the surface charge that was found to dominate the attachment phenomena in sand packed columns. Techniques also revealed a probable role of other cell surface macromolecules (LPS) that could account for non-DLVO behaviour. The results illustrate the importance of considering physicochemical conditions relevant to the natural subsurface environment when designing laboratory transport experiments as evidenced by variations in microbe migration as a function of the DO under growth and acclimation.

*Keywords:* bacterial adhesion, bacterial transport, DLVO, physicochemical characterization, dissolved oxygen, porous media.

## RÉSUMÉ

Les propriétés caractéristiques de la surface des cellules bactériennes ont une grande influence sur l'adhésion des bactéries sur les surfaces. La protection de l'eau potable exige une meilleure compréhension des facteurs contrôlant la migration des bactéries qui causent des maladies. Cette étude a investigué le comportement migratoire des bactéries pathogéniques couramment menaçantes dans des systèmes granulaires saturées d'eau. Ces deux bactéries facultatives sont l'*Escherichia coli* O157:H7 et le *Yersinia enterocolitica*. Ils ont tous les deux été développées dans des environnements aérobie et anaérobie suivit d'une période d'adaptation de 21 heures dans un environnement aquatique entièrement aéré. Les expériences de laboratoires ont été conduites en écoulant les bactéries, suspendues dans des électrolytes ayant des concentrations d'oxygène dissout soit hautes ou basses dans des colonnes contenant des granules saturées avec l'électrolyte approprié. Les différences dans les résultats obtenus ont permit d'observer que le potentiel de transport des pathogènes dépend amplement sur la quantité d'oxygène dissout dans leur environnement de développement et durant la période d'adaptation. D'autres analyses des caractéristiques des microbes faites en effectuant des titulations cellulaires et des spectroscopies infrarouges à transformée de Fourier (FTIR), ont contribuées a mieux comprendre la source des charges sur la surface des cellules. D'après les résultats obtenus, ceux-ci ont joué un rôle dominant dans le phénomène d'adhésion des bactéries sur les graines de sables contenues dans les colonnes. Ces techniques démontrent aussi le rôle probable d'autres macromolécules situées sur la surface cellulaire pouvant contribués au comportement non-DLVO. Tous ces résultats illustrent l'importance de prendre en considération les conditions physicochimiques,

semblables aux surfaces souterrain de l'environnement naturel, durant la planification des expériences de laboratoires concernant le transport bactérien, puisqu'il a été clairement observé que la migration des microbes varie selon la concentration d'oxygène dissout durant le développement et la période d'adaptation.

*Mots clés* : adhésion bactériennes, transport bactérien, DLVO, caractérisation physicochimique, oxygène dissout, environnement poreux.

## ACKNOWLEDGMENTS

First, I would like to acknowledge the support of my thesis supervisor, Professor Nathalie Tufenkji, her great assistance and guidance throughout the period of my Masters degree and giving me the opportunity to start this journey.

The financial support from the following agencies made this research possible: the Fonds québécois de la recherche sur la nature et les technologies (FQRNT Team Grant), the Centre for Host-Parasite Interactions at McGill (New Initiatives Grant), the Canadian Water Network (CWN), NSERC, and the Canada Foundation for Innovation (CFI).

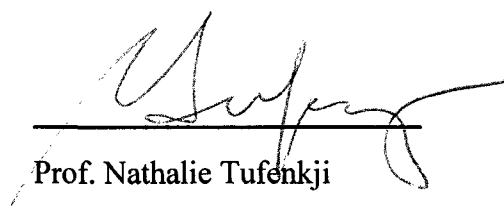
During my time at McGill I had the pleasure to meet wonderful people and have the opportunity to work by their side. From my lab group thanks to Charles Poitras, Ivan Quevedo, Andrew Pelley, Caroline Warne, Irwin Eydelnant for the daily fun and moral support.

Big thanks to my very supportive, encouraging and understanding family and friends. Thanks to Nadia for sharing with me that greatest passion for life.

## CONTRIBUTION OF AUTHORS

This thesis work is divided into two manuscripts (to be submitted). Authorship of the first article titled “*Role of Oxygen Tension on the Transport and Retention of Pathogenic Bacteria in Saturated Porous Media*” is Felipe Castro and Nathalie Tufenkji. Authorship of the second article titled “*Effect of Dissolved Oxygen on Physicochemical Properties of Selected Pathogenic Bacteria*” is Felipe Castro, Ashraf Ismail, and Nathalie Tufenkji.

Experimental work was conducted by Felipe Castro, as well as the analysis of the data and the writing of the draft manuscripts. Dr. Ismail supported with analysis of the infra-red spectra and helped throughout editing Chapter 3. Dr. N. Tufenkji helped throughout in supervision of experiments and editing the manuscript text.



---

Prof. Nathalie Tufenkji



---

Prof. Ashraf Ismail

# TABLE OF CONTENTS

	Page
ABSTRACT.....	ii
RÉSUMÉ .....	iii
ACKNOWLEDGMENTS .....	v
CONTRIBUTION OF AUTHORS.....	vi
LIST OF FIGURES .....	ix
LIST OF TABLES .....	x
CHAPTER 1 .....	1
Introduction.....	1
1.1 Groundwater Microbial Contamination .....	1
1.2 Bacteria as Colloids.....	2
1.3 Electrostatic Forces .....	2
1.4 Colloid Filtration Theory .....	5
1.5 Thesis Objectives .....	6
1.6 Thesis Layout .....	7
1.7 Literature cited .....	9
CHAPTER 2 .....	10
ROLE OF OXYGEN TENSION ON THE TRANSPORT AND RETENTION OF PATHOGENIC BACTERIA IN SATURATED POROUS MEDIA .....	10
2.1 Abstract .....	10
2.2 Introduction .....	11
2.3 Materials and Methods .....	13
2.3.1 Experimental Design.....	13
2.3.2 Bacteria Selection and Growth Protocols .....	14
2.3.3 Bacterial Cell Acclimatization .....	14
2.3.4 Bacterial Cell Characterization .....	16
2.3.5 Bacterial Transport and Deposition Experiment.....	17
2.3.6 Interpretation of Bacterial Column Experiments.....	18

2.4	Results and Discussion .....	19
2.4.1	Characterization of Bacterial Cells .....	19
2.4.2	Effect of Oxygen Tension during Growth on Bacterial Transport and Retention .....	25
2.4.3	Effect of Oxygen Tension during Acclimatization on Bacterial Transport in Packed Column .....	27
2.4.4	Linking Bacterial Transport Behaviour to Cell Properties .....	28
2.5	Environmental Implications .....	30
2.6	Acknowledgements .....	32
2.7	Literature Cited .....	33
CHAPTER 3 .....		37
EFFECT OF DISSOLVED OXYGEN ON THE PHYSICOCHEMICAL PROPERTIES OF SELECTED PATHOGENIC BACTERIA .....		37
3.1	Abstract .....	37
3.2	Introduction .....	38
3.3	Materials and Methods .....	41
3.3.1	Experimental Design .....	41
3.3.2	Bacteria Selection and Growth Protocols .....	41
3.3.3	Bacteria Acclimation Protocol .....	42
3.3.4	ATR-FTIR Spectroscopy .....	43
3.3.5	Bacterial Cell Characterization .....	44
3.3.6	Titrations of Bacteria Cells .....	44
3.4	Results and Discussion .....	47
3.4.1	Electrokinetic Characterization of Bacteria .....	47
3.4.2	Potentiometric Titrations .....	48
3.4.3	ATR-FTIR spectroscopy .....	52
3.5	Environmental Implications .....	57
3.6	Literature Cited .....	59
CHAPTER 4 .....		64
Conclusions .....		64
APPENDIX .....		65

# LIST OF FIGURES

Page

FIGURE 2.1: Measured bacterial electrophoretic mobilities (EPM) shown as open symbols (left y-axis), and measured bacterial attachment efficiencies ( $\alpha$ ) shown as a bar plot (right y-axis) for (a) <i>E. coli</i> O157:H7 and (b) <i>Y. enterocolitica</i> . Four treatments were considered: (i) ANALow (cells grown anaerobically, then acclimated in lowDO electrolyte); (ii) AERlow (cells grown aerobically, then acclimated in lowDO electrolyte); (iii) ANAsat (cells grown anaerobically, then acclimated in satDO electrolyte); (iv) AERsat (cells grown aerobically, then acclimated in satDO electrolyte). Data represent the mean $\pm$ 95% confidence interval. ....	21
FIGURE 2.2: Shape descriptors for both cell types obtained by image analysis. (a) and (b) equivalent spherical diameter based on the volume of a spheroid (spheroid length and width determined from object projection). (c) and (d) cell aspect ratio (cell length divided by cell width). Data represent the mean $\pm$ 95% confidence interval. ....	23
FIGURE 2.3: Surface charge per cell determined from the amount of NaOH consumed during titration of bacteria (suspended in $10^{-2}$ M KCl) from pH 4.0 to 9.5. Data represent the mean $\pm$ 95% confidence interval. ....	25
FIGURE 3.1: Concentration of titrated charged sites at pH 6.7 following the four treatments for (a) <i>E. coli</i> O157:H7 and (b) <i>Y. enterocolitica</i> (bar graph). Box plots represent the zeta potential. ....	48
FIGURE 3.2: <i>E. coli</i> (a) and <i>Yersinia</i> (b) spectra (bottom curves) obtained by difference spectra analysis between aerobic and anaerobic growth for cells acclimatized under low DO at pH 6.7. Differences can be seen at the phosphate and polysaccharide ( $950-1200\text{ cm}^{-1}$ ) bands. For further reference see table 3.3. ....	55
FIGURE 3.3: Integrated intensity of carbohydrate IR ( $950-1200\text{ cm}^{-1}$ ) band for both bacteria suspended in KCl 10 mM at pH 6.7. The bands have been normalized to the amide II band. Bars include 95% confidence interval. ....	56

## LIST OF TABLES

	Page
TABLE 3.1: $pK_a$ values and their corresponding site concentrations ( $S_i$ ) for <i>E. coli</i> O157:H7 and <i>Y. enterocolitica</i> . Values in parentheses are one standard deviation of two experiments. Variance (goodness of fit) as calculated by FITEQL 4.0.....	<b>49</b>
TABLE 3.2: Functional groups and corresponding IR absorption frequencies encountered in both bacteria strains. Band assignment extracted from Naumann 2000, Dittrich and Sibling 2006 & 2005, Yee et al 2006 and Turney et al 2006. ....	<b>53</b>

# CHAPTER 1

## Introduction

### 1.1 Groundwater Microbial Contamination

The World Health Organisation (WHO) has identified that pathogen contamination continues to be the greatest risk to the quality of drinking water supplies [1]. Worldwide, groundwater accounts for nearly 90% of the world's readily available freshwater resources [2]; in Canada alone, nearly 9 million people rely on groundwater for domestic use [3]. The contamination of underground fresh water resources by microbial pathogens and parasites as a result of wastewater infiltrating into the soil that recharges groundwater via leaking sewage systems, leakage from manure or livestock wastes, wastewater or sewage sludge spread by farmers on fields, leakage from waste disposal sites and landfills, or artificial recharge of treated wastewater is of increasing concern. If the distance from point of pollution to point of freshwater extraction is relatively small, there is a real likelihood of withdrawal of pathogenic microbes. A study reported in 2000 that developing countries such as Asia, South America and Africa have an estimated 1,300 million people living in urban areas, for whom the main source of drinking water is groundwater [4]

Recent studies have revealed the importance of natural climate events as potential sources of groundwater contamination. In Canada, the Walkerton tragedy that resulted in the death of 6 people and left over 700 sick due to *E. coli* O157:H7 contamination in a water supply was preceded by a heavy rainfall event. It has been also demonstrated that after heavy rainfalls in the US, outbreaks due to surface water contamination showed the

strongest association with extreme precipitation during the month of the outbreak and a 2-month lag applied to groundwater contamination events [5].

## **1.2 Bacteria as Colloids**

The definition of colloids includes particles that are small enough to remain in suspension, though not so small that they actually dissolve in solution. The generally accepted size range of particles that can exhibit both these behaviours is fairly wide, from a few nanometers to around 50  $\mu\text{m}$ . Colloidal suspensions can be found in everyday life, from paint, to ink in inkjet printers, to milk, and toothpaste. Because most bacteria are between 1 and 10 microns in size, they also can be considered to be colloids [6]. Because of this fact, the typical theories and equations of colloidal science have been applied to bacterial systems, with varying degrees of success

## **1.3 Electrostatic Forces**

The Derjaguin-Landau-Verwey-Overbeek (DLVO) theory of colloidal stability predicts that the total interaction energy between a colloid and a surface in aqueous media is dependent upon a number of factors, including surface potential. To determine whether the behaviour of bacterial suspensions during filtration experiments can be explained by electrostatic forces, it is necessary to characterize the surface potential of bacteria. Since direct measurement of the surface potential of a colloid is difficult, indirect measurements of surface potential are often used instead and one such measure is known as the zeta potential ( $\zeta$ ). Zeta potential can be determined by making use of a process known as Laser Doppler Velocimetry (LDV) in conjunction with Phase Analysis Light Scattering (PALS) [7].

The electrostatic charges on microbial surfaces in solution are caused by dissociation of various inorganic acid-base functional groups, such as carboxyl, phosphoric and amino groups, located at the outer surface membrane. For most bacterial species, the isoelectric point lies between pH 1.5 and 4.0 [8], giving bacteria in a natural environment (pH about 7) a net negative surface potential (negative  $\zeta$ -potential). The dissociation of an acidic functional group results in a negatively charged surface. The net surface charge of a particle is then a function of the relative strengths of its various acidic and basic functional groups and of the pH of the solution.

The development of a net charge at the surface of the bacteria affects the local distribution of ions and leads to the development of a boundary layer with a higher concentration of counter ions than that of the bulk phase. The inner region is known as the Stern layer and within this region ions are very strongly associated with the surface whereas the ions in the outer region, known as the diffuse layer, are much less firmly associated [9]. Within this diffuse layer there exists a notional boundary in which the ions inside that boundary remain associated with the particle as it travels through the medium. This boundary acts as the surface of hydrodynamic shear for the colloidal particle (bacteria) and the electrical potential at this boundary is known as the  $\zeta$ -potential.

An important property of charged bacteria and colloidal particles in general is their tendency to interact with an applied electric field. These interactions are collectively referred to as electrokinetic effects. As charged particles suspended in an electrolyte are subjected to an applied electric field, they will have an affinity to the oppositely charged electrode. The velocity of a particle in an electric field is called its *electrophoretic mobility* (equation 1) and can be related to the  $\zeta$ -potential of a particle through use of the Henry equation [6]:

$$U_{\varepsilon} = \frac{2 \varepsilon \zeta f(\kappa a_p)}{3 \eta} \quad (1)$$

where  $U_{\varepsilon}$  = electrophoretic mobility,  $\varepsilon$  = dielectric constant of the solution,  $\zeta$  = zeta potential, and  $f(\kappa a_p)$  is the Henry's function (dependent upon  $\kappa$  = Debye length and  $a_p$  = particle radius). The reciprocal of the Debye length is often thought of as being the "thickness" of the electrical double layer. Well known approximations are often used when determining the appropriate value of the Henry's function. For the common case of particles larger than 0.2 microns dispersed in more than  $10^{-3}$  molar 1:1 electrolyte, the Smoluchowski approximation is used and the Henry's function is taken as 1.5. For small particles in the presence of less than  $10^{-3}$  molar 1:1 electrolyte, the Huckel approximation is used and 1.0 is used for the Henry's function. In other words, when the thickness of the electrical double layer is small relative to the size of the particle the Smoluchowski approximation is used and when particle size is small relative to the EDL thickness, the Huckel approximation is used [6]. In addition to surface charge, the magnitude of the electrophoretic mobility is also controlled by the concentration of electrolyte ions in solution. At high electrolyte concentrations, electrostatic sorption of counter-ions can satisfy the excess surface charge and decrease surface electric potential. In contrast, dilute electrolyte concentrations allows the surface electric field to expand which results in increasing electrophoretic velocities.

## 1.4 Colloid Filtration Theory

The migration of bacterial pathogens through porous media can be estimated through the use of colloidal filtration transport models. The first transport model, the classic filtration model, was developed by Yao *et al.* [10], however this model does not take certain forces into account such as hydrodynamic interactions and van der Waals attractive forces [11]. To cope with these limitations, recent computational approaches have been developed that incorporate more interactions. A correlation equation was developed by Rajagopalan and Tien [12], however, this correlation did not take into account the hydrodynamic interactions and van der Waals attractive forces on particles undergoing Brownian diffusion. Another more recent correlation equation was recently developed by Tufenkji and Elimelech which is referred to as the TE equation which takes into account the forces and interactions excluded by the previous correlation equations, thus providing a more accurate prediction [11]

The classic filtration model was developed by Yao *et al.* and it is derived from a mass balance on the transport of a single colloidal particle traveling through a porous media [10]. The integrated form of this general mass balance is:

$$\ln \frac{C}{C_0} = -\frac{3}{2}(1-f)\alpha\eta_0 \left( \frac{L}{d_c} \right) \quad (2)$$

where  $C$  is the effluent concentration,  $C_0$  is the influent concentration,  $f$  is the bed porosity,  $\alpha$  is the attachment efficiency factor,  $\eta_0$  is the single-collector contact efficiency,  $L$  is the bed depth and  $d_c$  is the diameter of the collector grain. The term  $\alpha$  is a ratio between the number of collisions between a colloidal particle and a collector grain that result in attachment divided by the total number of collisions. For  $\alpha = 1$ , all collisions result in attachment, whereas if  $\alpha = 0$ , then attachment does not occur. The term  $\eta_0$  is a

ratio between the rate at which colloidal particles collide with the collector grain divided by the rate at which colloids flow to the collector grain. This term measures the ratio of colloids that come into contact with a collector grain.

The three main mechanisms governing the transport of the particle include:

- i) Interception: colloid flowing along a stream line and colliding with a collector grain because of its size;
- ii) Sedimentation or gravity: effects of buoyancy and fluid drag on the colloid; and
- iii) Diffusion: Brownian movement of the colloid.

An analytical expression for  $\eta_0$  is represented by:

$$\eta_0 = \eta_D + \eta_I + \eta_G$$

where  $\eta_D$  is the transport by diffusion,  $\eta_I$  is the transport by interception, and  $\eta_G$  is the transport by gravity [10]. The original expressions for  $\eta_D$ ,  $\eta_I$ , and  $\eta_G$  proposed by Yao *et al.* have been updated most recently by Tufenkji and Elimelech in the development of the TE equation [11].

## 1.5 Thesis Objectives

The principal objective of this thesis work is to examine the role of dissolved oxygen on microbial migration in water saturated granular systems (porous media), a model system mimicking an aquifer. There is limited information in the literature regarding attachment behaviour of pathogenic bacteria to porous media in response to antecedent oxygen availability during culture. Likewise, we found no study addressing metabolic changes or environmentally-driven adaptations (non-evolutionary) that can influence mobility in porous media as a function of the environmental dissolved oxygen level. In addition,

there is no work to date addressing the role of dissolved oxygen during transport itself in porous media. To address these questions, we have customized a common microbial transport test (sand packed columns) commonly used to characterize kinetics of adsorption in order to examine more relevant conditions found in the subsurface. The system is able to keep a steady temperature of 11 °C and known electrolyte dissolved oxygen concentration during acclimation (21 h) and transport through the laboratory-scale sand-packed columns. The goal is to address under which conditions selected bacterial pathogens would have enhanced abilities to migrate in aquifers or groundwater environments.

Other main objective is to try to identify the controlling mechanisms involved in the interactions between bacteria and sand surfaces. After measuring a detectable macroscopic effect of dissolved oxygen using colloid filtration theory, it is of interest to reveal what is causing, in the worst case scenario, the detrimental adhesive properties. To this end, we have conducted electrophoretic mobility measurements to assess the role of electrostatic interactions, bacteria cell titrations in order to quantify the amount of charge and FTIR spectra analysis to try to further identify cell surface functional groups and macromolecular species associated with the main controlling elements during transport. The investigation is performed within the context of the DLVO theory of colloid stability and colloid filtration theory.

## **1.6 Thesis Layout**

Chapter 2 reports well-controlled laboratory-scale column deposition experiments of two selected bacterial pathogens at 11°C and pH 6.7. The results provide evidence of the direct effect of extreme dissolved oxygen concentrations studied during growth

(anaerobic and aerobic) and acclimation for 21h (microaerophilic and saturated) on bacterial retention in granular porous media. Special attention is given to electrostatic-type interactions accounted for by electrophoretic mobility (EPM) measurements. Size and shape as a function of growth and acclimation is also considered and characterized using microscopy techniques.

The focus of Chapter 3 is to examine the source of the observed deposition behaviour at a molecular level. Special attention is given to the source of the electrostatic charge at the bacterial surface that was found to predominate in the experiments presented in Chapter 2. Macroscopic methods, such as titration of bacterial cells along with the modeling of the experimental data are utilized to find the major proton-active functional groups and the overall cell surface charge at the outer bacterial membrane. The Attenuated Total Reflectance Fourier Transform infrared (ATR-FTIR) spectroscopy technique was used to examine the interfacial properties of the cells in order to reveal the active functional groups and macromolecular structures that might be involved in the development of the charge and adhesive behaviour of the pathogens studied.

## 1.7 Literature cited

1. WHO/UNICEF. *Meeting the MDG Drinking Water and Sanitation Target: A Mid-Term Assessment of Progress*. 2004. Geneva.
2. Environment Canada, *Water - Here, There and Everywhere*. 2002.
3. Statistics Canada, *Special compilation using data from Environment Canada, Municipal Water Use Database*. 1996, Statistics Canada, Environment Accounts and Statistics Division, Ottawa. p. 11-3.
4. United Nations, World Bank and World Resources Institute, *A guide to world resources 2002*.
5. Curriero FC, P.J., Rose JB, Lele S., *The association between extreme precipitation and waterborne disease outbreaks in the United States 1948-1994*. Am J Public Health, 2001. **91**: p. 1194-1199.
6. M. Elimelech, J.G., X. Jia, R. A. Williams, *Particle Deposition & Aggregation: Measurement, Modeling and Simulation* ed. Butterworth-Heinemann. 1995.
7. Morfesis, A., Watson, L., Fraser, M., , *Zetasizer Nano Z/ZS Training Course*, in *The Zeta Potential*. 2006, Malvern Instruments: USA.
8. Harden V, H.J., *The isoelectric point of bacterial cells*. J Bacteriol, 1953. **65**: p. 198-202.
9. Verwey, E.J.W., Overbeek, J.Th.G., *Theory of the Stability of Lyophobic Colloids*. 1948.
10. Yao, K.M., M.M. Habibian, and C.R. Omelia, *Water and Waste Water Filtration - Concepts and Applications* Environmental Science & Technology, 1971. **5**(11): p. 1105-&.
11. Tufenkji, N. and M. Elimelech *Correlation equation for predicting single-collector efficiency in physicochemical filtration in saturated porous media*. Environmental Science & Technology, 2004. **38**(2): p. 529-536.
12. Rajagopalan, R.T., C., *Trajectory Analysis of Deep-Bed Filtration with Sphere-in-Cell Porous-Media Model*. Aiche Journal, 1976. **22**(3): p. 523-533.

## CHAPTER 2

# Role of Oxygen Tension on the Transport and Retention of Pathogenic Bacteria in Saturated Porous Media

### 2.1 Abstract

To examine the influence of variations in dissolved oxygen (DO) concentration on pathogen mobility, laboratory-scale filtration experiments were performed using the enterohemorrhagic strain *Escherichia coli* O157:H7 and the enteroinvasive organism *Yersinia enterocolitica*. Cells were incubated either in the absence (anaerobic) or presence (aerobic) of oxygen to understand how variations in DO during growth may affect bacterial transport and retention in water saturated granular porous media. The influence of DO during growth is found to be organism dependent, whereby *E. coli* O157:H7 exhibits decreased transport potential when grown in the presence of O<sub>2</sub> and *Y. enterocolitica* exhibits greater transport when grown aerobically. To understand the influence of DO changes during cell acclimatization and transport, bacteria were resuspended and acclimatized in either oxygen depleted (low DO) or oxygen rich (saturated DO) electrolytes prior to conducting filtration experiments. The effect of DO on bacterial transport and retention is shown to be dependent on antecedent growth conditions and on the organism studied. Measurements of cell surface charge, shape and size reveal notable variability when oxygen tension is changed during bacterial growth or acclimation and are linked to the observed bacterial transport behavior.

## 2.2 Introduction

Microbial transport and deposition in granular porous media is of interest in a broad range of environmental applications, including in-situ bioaugmentation (1), riverbank filtration (2), and engineered water treatment systems (3). Adequate protection of potable water supplies and effective treatment of contaminated soils or waters necessitate predictive models of microbe migration in granular matrices. Such mathematical models of microbial fate and transport require a mechanistic understanding of the key processes or factors controlling microbe migration, retention, and survival in varied natural and engineered aqueous environments. Consequently, over the past thirty years, more than 100 laboratory or field studies have been aimed at improving our knowledge of the chemical, physical, and biological factors influencing the migration of microorganisms in granular porous media (4, 5). More recently, with increasing concerns over contamination of potable water supplies by microbial pathogens, studies have been conducted with toxigenic strains of bacteria such as *Escherichia coli* (*E. coli*) O157:H7 and infective parasites (e.g., *Cryptosporidium*) (6, 7). Nonetheless, there remain important gaps in our understanding of microbe behavior that limits our ability to predict microbial transport and fate in aqueous systems.

Baseflow groundwater can be anoxic or hypoxic with dissolved oxygen (DO) concentrations commonly ranging between 0 and 0.95 mg DO/L (8). Higher DO values can be observed in shallow and unconfined aquifers, turbulent groundwater, and aquifers directly connected to aerobic surface waters (9). In environments such as alluvial aquifers used in riverbank filtration, varying DO levels are commonly observed due to facultative microbial activity through soil strata and reaeration at the soil surface (2).

Aquifer recharge activity, heavy rainfall events and stormwater infiltration may also disturb groundwater chemistry and the composition of dissolved gases in the subsurface (10). For instance, it has been shown that cold winter stormwater can slightly re-oxygenate groundwater in shallow aquifers, whereas warm summer stormwater may lower DO concentrations in groundwater at depths of 2 to 3 meters (10). In engineered water treatment systems (e.g., deep-bed granular filtration or trickling filters), the concentration of DO can also fluctuate along the flow path of the treated water.

Although it is known that water oxygen tension can exhibit temporal and spatial variability in natural and engineered granular matrices, studies examining the influence of oxygen tension on microbe migration in these environments are scarce. Some earlier studies have been aimed at investigating the mechanisms controlling microbial colonization of granular porous material under static conditions in an anaerobic environment most relevant to deep aquifers with very slow groundwater velocities (11, 12). Yang (13) evaluated the transport behavior of multiple *E. coli* isolates, as well as a nonpathogenic O157:H7 strain, in different granular materials when grown under anaerobic or aerobic conditions. This study demonstrated important variability in cell surface properties between the different isolates and showed how the growth conditions strongly influenced the surface properties, biofilm formation potential, and migration behavior of the organisms (13, 14). Overall, the environmental *E. coli* isolates examined exhibited increased retention when grown under aerobic conditions. Similarly, in a recent investigation of *E. coli* W3100 transport and retention in sand packed columns, it was shown that anoxia is a negative environmental signal for attachment of this organism to sand (15). This finding was linked to the observation that growth under oxygen-limited conditions leads to increased expression of the *fliC* gene (encoding major flagellar subunit

FliC) and overproduction of lipopolysaccharide (LPS). The abovementioned studies have begun to address the effect of anaerobic growth on *E. coli* migration; however, variations in DO concentrations during bacterial transport have not been taken into consideration. In certain cases, the bacteria of interest may grow in an anaerobic environment (e.g., the intestinal tract of wildlife or farm animals) but migration can take place in oxygen-rich waters. The opposite is also true, whereby cells may proliferate in an aerobic atmosphere (e.g., the uppermost soil layers and open water bodies) but subsequently be released to an anaerobic or hypoxic environment. Although these different scenarios are likely encountered in natural and engineered aqueous systems, research examining the influence of variable DO concentrations during bacterial growth and acclimation is lacking.

The general objective of this study is to investigate the sensitivity of pathogenic bacteria to variations in oxygen tension during (i) growth or (ii) acclimation and transport. The selected enteric pathogens *E. coli* O157:H7 and *Yersinia enterocolitica* (*Y. enterocolitica*) were grown in the absence (anaerobic) or presence (aerobic) of O<sub>2</sub>, then resuspended in oxygen rich or oxygen depleted electrolytes to examine the effect of this environmental parameter on bacterial migration potential. Electrokinetic and physical properties of the two organisms characterized over the range of conditions examined are used in the interpretation of data obtained from the packed column experiments.

## **2.3 Materials and Methods**

### **2.3.1 Experimental Design**

Four treatments were considered that examined the influence of oxygen tension during bacteria growth and acclimation on bacterial transport. Selected bacteria were grown either anaerobically (ANA) or aerobically (AER), then resuspended in a prepared

electrolyte solution (10 mM KCl) of either low dissolved oxygen (lowDO) or saturated dissolved oxygen (satDO) concentration. Additional details regarding the preparation of the electrolyte solutions are provided below. Following a 21 h acclimation period in the lowDO or satDO electrolyte solution at 9 °C, bacterial transport was examined using column transport experiments conducted at 11 °C.

### **2.3.2 Bacteria Selection and Growth Protocols**

Two pathogenic Gram-negative microorganisms were selected for this study, *Escherichia coli* O157:H7 ATCC 700927 and *Yersinia enterocolitica* ATCC 23715. Pure cultures were maintained at -80 °C in Luria-Bertani Lennox broth (20 g/L, Fisher) with 15% glycerol. One day prior to inoculation, frozen cultures were streaked onto solid LB agar plates that were then incubated at 37 °C for 21 h. For each bacterial transport experiment, a colony from the starter plate was used to inoculate sterile LB broth. Aerobic (AER) growth for both strains involved incubation at 37 °C and 200 rpm for 8 h in 150 mL of LB broth (in a 500 mL baffled flask), at which point the cells were harvested. Anaerobic (ANA) growth for both strains involved incubation at 37 °C in 200 mL of LB broth in capped 250 mL centrifuge bottles (Nalgene) maintained without agitation for 20 h.

### **2.3.3 Bacterial Cell Acclimation**

Following the selected growth protocol (AER or ANA), the cell culture was centrifuged (Sorvall RC6) for 15 min at 5860g in an SS-34 rotor (Kendro). The growth medium was decanted and the pellet was resuspended in freshly prepared electrolyte (either lowDO or satDO 10 mM KCl solution). To remove all traces of the growth medium, the cells were centrifuged and resuspended in fresh electrolyte one additional time. Analytical reagent grade KCl, KHCO<sub>3</sub>, KOH and HCl (Fisher) and deionized (Milli-Q) water (DI) were used

to prepare the electrolyte solutions. The satDO electrolyte was prepared by vigorous stirring and sparging of 1.2 L KCl solution (10 mM) using filtered (Durapore PVDF membrane, 0.22  $\mu\text{m}$ , Millipore) air at 1.8 vvm in a 2 L Erlenmeyer flask for 30 min. The final DO level of the satDO solution was  $8.6 \pm 0.3$  mg DO/L. The lowDO electrolyte was prepared by vigorously stirring and sparging a 1.2 L KCl solution (10 mM) with prepurified  $\text{N}_2$  at 1.8 vvm in a tightly capped 2 L Erlenmeyer flask for 30 min. The final DO level of the lowDO electrolyte was  $0.4 \pm 0.3$  mg DO/L. Prepared lowDO or satDO electrolytes were transferred to a 2 L low gas permeability bioprocess bag (Labtainer, Hyclone) using a glass tube positioned at the bottom of the 2 L flask. After transfer of the lowDO or satDO electrolytes to the Labtainer bag, the total equivalent dissolved  $\text{CO}_2$  concentration was adjusted to  $\sim 1.2 \times 10^{-5}$  M using 0.1M  $\text{KHCO}_3$  (Fisher) and the pH was adjusted to  $6.7 \pm 0.2$  using 0.1 M HCl or 0.1 M KOH (Fisher). Washed cells were resuspended to a final concentration of  $\sim 4 \times 10^7$  cells/mL in either lowDO or satDO electrolyte contained in a separate 500 mL Labtainer bag. The Labtainer bags holding the washed cells (bacteria suspension, 500 mL bag) and the bacteria-free electrolyte (background solution, 2 L bag) were then maintained at  $9^\circ\text{C}$  for 21 h. This cold temperature acclimation was used to replicate conditions that may be encountered by cells following release into groundwater representative of the Canadian climate. Actual DO levels of the background solution and bacteria suspension were verified using a micro flow-through polarographic DO probe (Model DO-166FT, Lazar Labs) connected to each Labtainer bag. In all four treatments, the cells were exposed to the same temperature and chemistry shifts when transferred from the incubation phase to the acclimation/transport phase; namely, cells were all incubated at  $37^\circ\text{C}$  in LB and all acclimated at  $9^\circ\text{C}$  in KCl solution.

Loss of cell viability during acclimation in the conditioned electrolytes at 9°C was verified using the BacLight Viability Kit (Molecular Probes, Eugene, OR). This technique involves direct counting of stained live and dead cells using a fluorescent microscope (IX-71, Olympus). Cell viability during acclimation for the four treatments examined was found to be greater than 92% and 83%, for ATCC 700927 and 23715, respectively.

#### **2.3.4 Bacterial Cell Characterization**

The nominal size and shape of the bacteria was determined by analyzing images of cells attached onto an amino-silanized glass slide in an inverted fluorescent microscope operating in phase contrast mode (60× magnification). For each sample, at least 600 individual cells were analyzed using ImageJ software (NIH) to determine the average lengths of the major and minor axes of the cells, the resulting equivalent spherical diameter, and cell aspect ratio (length divided by width).

Microelectrophoresis (ZetaSizer Nano ZS, Malvern) was used to characterize the electrokinetic properties of the cells. Electrophoretic mobility (EPM) was measured at 11 °C using the actual cell suspensions ( $\sim 4 \times 10^7$  cells/mL) to be used for the transport experiments. These measurements were repeated using at least three different fresh bacterial suspension samples, measured at least 3 times each.

Potentiometric titrations were conducted to determine the relative acidity of the bacterial surfaces. Bacterial suspensions previously grown under different culture and acclimation protocols were resuspended in 10 mM KCl to a concentration of  $7.5 \times 10^9$  —  $4.0 \times 10^{10}$  cells/mL and stored at 9.0 °C inside Labtainer bags. After 21 h of acclimation, 50 mL of the bacterial suspensions were purged for 20 min with N<sub>2</sub> gas in a closed jacketed glass vessel maintained at 11 °C. Titrations were repeated at least twice starting

at pH 3.4 to 11.0 at 11 °C using a 798 Titrino automatic titrator (Metrohm Ltd.). The titrant solution (0.1N NaOH) was degassed for 30 min prior to titrations. Standardized degassed 0.1 N HCl was used to bring the pH to 3.4. The volume of NaOH consumed during a titration was used to determine the acidity of the cells and the corresponding surface charge density.

### **2.3.5 Bacterial Transport and Deposition Experiment**

Column experiments were conducted to evaluate the transport of the two organisms separately after acclimation in lowDO or satDO KCl solution. Experiments were conducted by pumping a bacterial suspension contained in a Labtainer bag through a glass column packed with clean electrolyte-saturated sand. An adjustable-height column (C 16/40, Amersham) with an inner diameter of 1.6 cm was used. The sand was wet-packed to a height of 89 mm with vibration. High purity (99.76% SiO<sub>2</sub>) quartz sand (Granusil #2040, Ottawa Plant, Unimin) was utilized as model granular media. The sand was size fractionated with nylon sieves (U.S. standard mesh sizes 20 and 25) and thoroughly cleaned to remove impurities. The cleaning steps included soaking the sand in 12 N HCl for 20 h, washing in DI water, repeating the acid soak and water rinse step, and baking at 800 °C for 6 h. Cleaned sand was stored in a dry glass bottle and rehydrated by soaking in the electrolyte of interest for 18 h at room temperature before packing the column. Microscopic examination of the sand grains revealed them to be well-rounded, and standard sieve analysis yielded an average grain diameter ( $d_{50}$ ) of 0.763 mm. Standard gravimetric methods were used to determine the sand density (2.62 g/cm<sup>3</sup>) and a column packing porosity of 0.35. The point of zero charge of quartz is ~ pH 2; hence, the overall charge on the sand grains is negative at the pH (6.7) of the experiments. The

column apparatus was placed inside a cold chamber maintained at 11 °C. Preparing cell suspensions at a slightly colder temperature (9 °C; see above) facilitated conducting the experiments at 11 °C (due to slight heat gain by the suspension during transfer to the chamber).

The conditions of the four treatments considered (ANALow, ANAsat, AERlow, and AERsat) were maintained for the transport phase of the experiment conducted in the packed column. Prior to each experiment, the packed column was equilibrated by allowing 40 pore volumes (PV) of the background electrolyte of interest held inside a 2 L Labtainer bag to flow through the column. The solution flow rate was maintained by a syringe pump (Model 200, KD Scientific) downstream of the column to retain an approach velocity of  $1.7 \times 10^{-4}$  cm/s. Next, a bacterial suspension of concentration ( $C_0$ )  $4 \times 10^7$  cells/mL of the same background electrolyte composition was flowed through the column for at least 4 PV followed by a bacteria-free electrolyte solution (4 PV) using the same pumping method described above. Bacterial cell concentration at the column outlet was monitored online with a UV/visible spectrophotometer (Hewlett-Packard Model 8453) using 1 cm flow-through cell (at 600 nm). Each experiment was conducted at least twice and good reproducibility was observed in the measured bacteria breakthrough curves. The DO level in the column effluent was monitored online using a flow-through DO probe to verify gas impermeability of the experimental apparatus. No significant changes in DO level were observed for all conditions.

### **2.3.6 Interpretation of Bacterial Column Experiments**

Classical colloid filtration theory (CFT) was used to quantitatively compare the bacterial attachment behavior to quartz sand in the four treatments examined. The attachment

efficiency ( $\alpha$ ) in CFT is a useful parameter to compare bacterial transport and deposition behavior observed under different conditions and was calculated from each breakthrough curve as follows [16]:

$$\alpha = -\frac{2}{3} \frac{d_c}{(1-\varepsilon)L\eta_0} \ln(C/C_0) \quad (1)$$

where  $d_c$  is the diameter of the sand grains,  $\varepsilon$  is the bed porosity,  $L$  is the bed length, and  $\eta_0$  is the theoretical single-collector contact efficiency evaluated using a correlation equation developed by Tufenkji and Elimelech [16]. Development of eq 1 assumes that the system under study is at steady-state and that bacterial detachment from the grain surface is negligible. The value of  $C/C_0$  in equation 1 was obtained from the experimental breakthrough curves (appendix ) during the initial (clean-bed) phase of bacterial elution.

## 2.4 Results and Discussion

### 2.4.1 Characterization of Bacterial Cells

Measured electrophoretic mobilities (EPM) of the two bacterial species for the four treatments considered in this study are presented in Figure 2.1 (open symbols). These data demonstrate the influence of the cell growth protocol (AER vs ANA) and cell acclimation protocol (lowDO vs satDO) on cell surface charge. Both cell types have a negatively charged surface in all four conditions examined. For *E. coli* O157:H7 (Figure 2.1a), the cells exhibit a greater absolute charge when grown in the absence of oxygen (ANA) versus those grown aerobically (AER). This observation is in agreement with measurements previously reported by Landini and Zehnder [15] showing more negative EPM for *E. coli* K12 mutants grown anaerobically in comparison to those grown aerobically. In contrast, Yang et al [14] found no significant differences in EPM for 14 *E. coli* isolates (including an O157:H7 strain) when grown anaerobically or aerobically. In

this latter study, however, the growth medium and incubation temperature were also different for the anaerobic and aerobic growth protocols. These differences in experimental protocols between the study of Yang et al (14) and the current study could have contributed to the observed opposite trend in EPM. The data shown in Figure 2.1a reveals that the cell acclimation process influences cell surface charge only for the *E. coli* grown anaerobically, where the average measured EPMs are -0.26 and -0.18  $\mu\text{m cm/V sec}$  for lowDO and satDO conditions, respectively. When *E. coli* O157:H7 is grown aerobically, the cell acclimation protocol does not affect the measured cell surface charge (at a 95% confidence level).

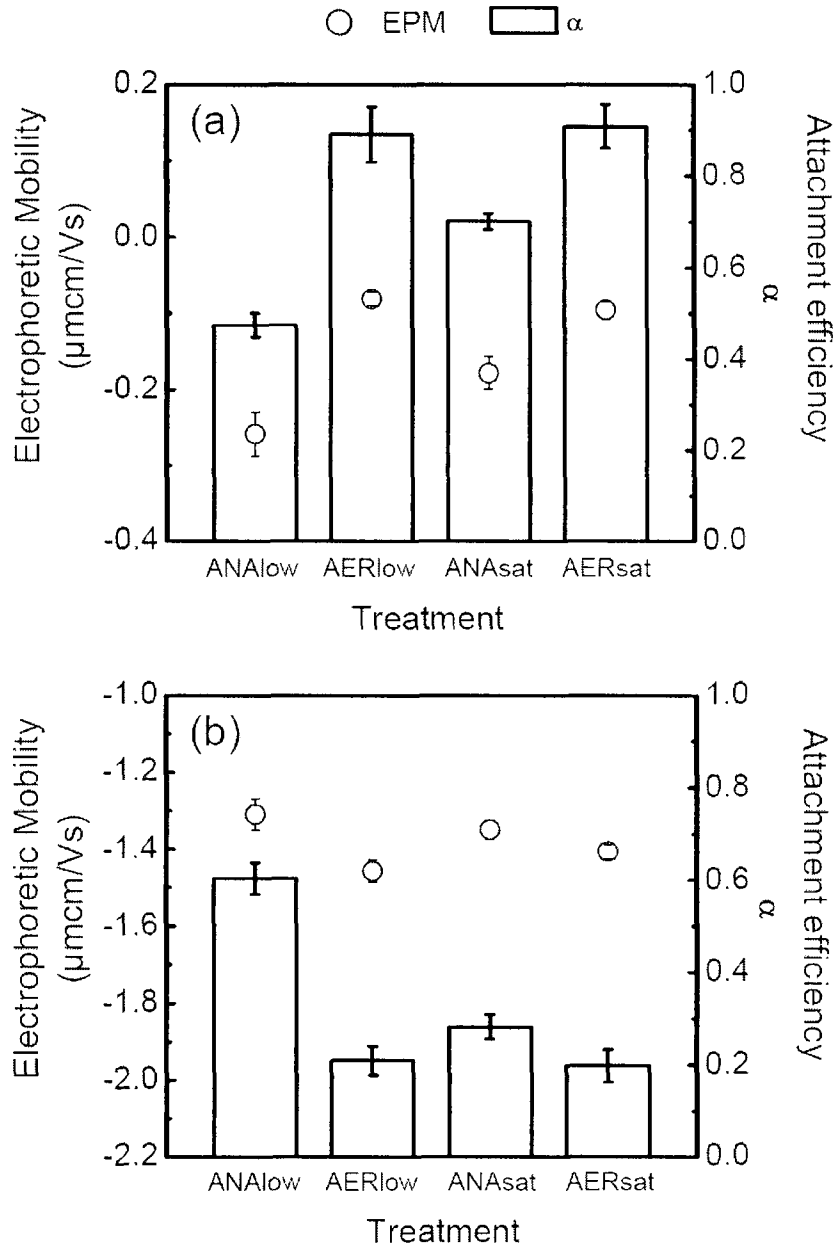


**FIGURE 2.1:** Measured bacterial electrophoretic mobilities (EPM) shown as open symbols (left y-axis), and measured bacterial attachment efficiencies ( $\alpha$ ) shown as a bar plot (right y-axis) for (a) *E. coli* O157:H7 and (b) *Y. enterocolitica*. Four treatments were considered: (i) ANALow (cells grown anaerobically, then acclimated in lowDO electrolyte); (ii) AERlow (cells grown aerobically, then acclimated in lowDO electrolyte); (iii) ANAsat (cells grown anaerobically, then acclimated in satDO electrolyte); (iv) AERsat (cells grown aerobically, then acclimated in satDO electrolyte). Data represent the mean  $\pm$  95% confidence interval.

The measured EPM for *Y. enterocolitica* is presented in Figure 2.1b (open symbols) for the four treatments considered. Overall, *Y. enterocolitica* exhibits a greater absolute charge than *E. coli* O157:H7 with average measured EPMs ranging between -1.5 to -1.3  $\mu\text{m cm/V sec}$  for the former, in comparison to values ranging between -0.26 to -0.08  $\mu\text{m cm/V sec}$  for the latter. In contrast to the results observed for *E. coli* O157:H7 (Figure 2.1a), *Yersinia* exhibits a greater absolute charge when grown in the presence of oxygen (AER) than when grown anaerobically (ANA). Moreover, when *Y. enterocolitica* is grown anaerobically, the cell acclimation protocol does not affect the measured cell surface charge (at a 95% confidence level). The data in Figure 2.1 provide insight on the influence of dissolved oxygen concentration on cell surface charge. The noted variations in cell EPM shown in Figure 2.1 are likely linked to physiological response of the cells resulting in different overall cell membrane composition (17, 18).

To examine the effect of variations in DO during cell growth and acclimation on cell size and shape, microscope images of cells adhered to amino-silanized slides were analyzed. The mean equivalent spherical diameter of the cells is presented in Figures 2.2a and b, whereas the mean cell aspect ratio (length/width) is shown in Figures 2.2c and d. *E. coli* O157:H7 has an average diameter of 0.69  $\mu\text{m}$  and does not exhibit any measurable differences in cell size for three of the treatments (ANALow, ANAsat, and AERlow) (i.e., the values are within the 95% confidence intervals of each other) (Fig 2.2a). The shape of this organism becomes more elongated when incubated under anaerobic conditions (Fig. 2.2c). Specifically, the average cell aspect ratio increases from 1.3 (AER) to 1.8 (ANA).

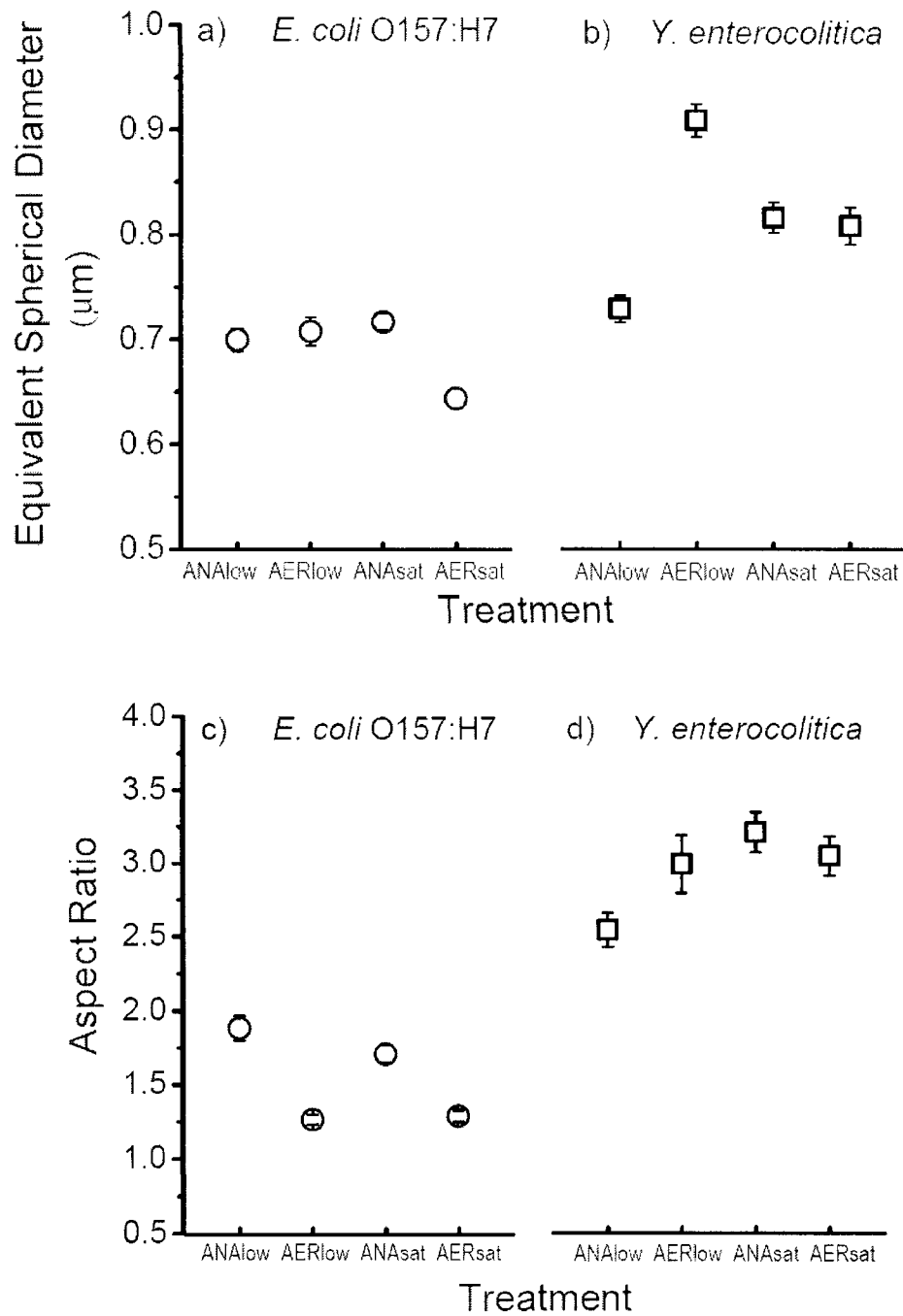


**FIGURE 2.2:** Shape descriptors for both cell types obtained by image analysis. (a) and (b) equivalent spherical diameter based on the volume of a spheroid (spheroid length and width determined from object projection). (c) and (d) cell aspect ratio (cell length divided by cell width). Data represent the mean  $\pm$  95% confidence interval.

*Y. enterocolitica* is larger in size and considerably more elongated than *E. coli* O157:H7 (at a 95% confidence level). The aspect ratio of *Y. enterocolitica* does not exhibit any detectable differences for three of the treatments (ANAsat, AERsat, AERlow) (Fig. 2d). The data in Figure 2.2 demonstrate how changes in oxygen tension during cell culturing and acclimation protocols may sometimes alter the physical properties of organisms. The shape and size of bacteria can play an important role in their transport and deposition in saturated granular porous media (19, 20) and the measurements presented here are used later in the paper to link bacterial cell properties to their migration behavior.

The results of potentiometric titrations of cell suspensions are presented in Figure 2.3. When the cells are grown anaerobically, *E. coli* and *Y. enterocolitica* exhibit comparable titratable cell surface charge. In the case of *E. coli* O157:H7, the number of dissociable functional groups on the cell surface is greater when the cells are grown in the absence of oxygen (ANA) (for the satDO treatment only). This observation is in qualitative agreement with the measured EPM for this treatment (Fig 2.1a) which indicates a greater absolute charge when the cells are grown anaerobically. *Y. enterocolitica* also exhibits differences in cell surface charge when grown aerobically or anaerobically (Figure 2.3). The surface charge per cell measured by potentiometric titration is greater for *Y. enterocolitica* grown in the presence of O<sub>2</sub> (i.e., AERsatDO > ANAsatDO, and AERlowDO > ANAlowDO at a 95% confidence level). Likewise, the absolute EPM is greater for *Y. enterocolitica* grown aerobically (Fig 2.1b). Inspection of Figure 2.3 also reveals that the acclimation of the bacteria in lowDO or satDO electrolyte influences the measured cell surface charge for cells grown aerobically (at a 95% confidence level). In an earlier study, Haas (21) noted significant differences in

functional group acid dissociation constants and site concentrations when culture conditions were changed from aerobic to anaerobic in the Gram negative organism *Shewanella putrefaciens*.

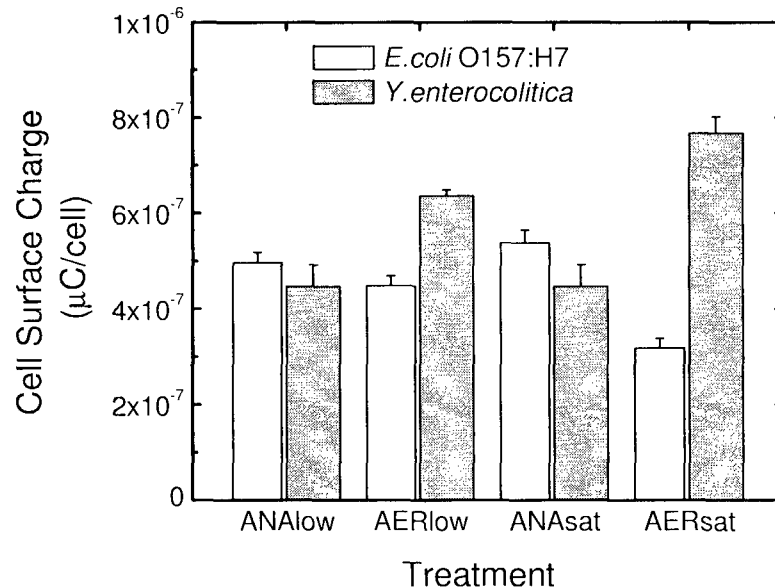


**FIGURE 2.3:** Surface charge per cell determined from the amount of NaOH consumed during titration of bacteria (suspended in  $10^{-2}$  M KCl) from pH 4.0 to 9.5. Data represent the mean  $\pm$  95% confidence interval.

#### 2.4.2 Effect of Oxygen Tension during Growth on Bacterial Transport and Retention

Column transport experiments were conducted to investigate the effect of aerobic (AER) versus anaerobic (ANA) growth conditions on the migration behavior of the two selected pathogenic Gram-negative strains. Bacterial attachment efficiencies ( $\alpha$ ) were calculated from the measured breakthrough curves (not shown) using eq 1 and are presented in Figure 2.1 in the form of bar graphs (right y-axis). *E. coli* O157:H7 exhibits a high extent of retention onto the clean sand grains ( $\alpha \approx 0.90$ ) when grown in the presence of oxygen (Fig. 2.1a). In contrast, incubation of *E. coli* O157:H7 under anaerobic conditions results

in decreased retention to the granular medium, with an average  $\alpha$  of 0.59. These results are in agreement with a previous study (15) examining the influence of oxygen tension during cell growth on the transport and adhesion of the nonpathogenic *E. coli* K12 in sand packed columns. These researchers also observed decreased bacterial adhesion when cells were grown under anaerobic conditions and demonstrated clear links between the observed reduction in adhesion and increased production of LPS and flagella (15). In an investigation of *E. coli* adhesion to various candidate biobarrier materials, Yang (14) also found decreased attachment when cells were grown in the absence of oxygen. Cell metabolism and gene expression will be affected by changes in oxygenation (22, 23). In the case of *E. coli*, it has been estimated that the expression of over one-third of the genes expressed during growth under aerobic conditions are altered when *E. coli* cells transition to an anaerobic growth state (24). Landini and Zehnder (15) demonstrated that the global regulatory *hns* gene plays a key role in controlling the adhesion behavior of *E. coli*. Anoxia has also been reported to hinder biofilm formation in *E. coli* K12 strains (25). However, further metabolic studies are required to better understand the global effect of oxygen deprivation on bacterial adhesion to surfaces.

Attachment efficiencies calculated for *Y. enterocolitica* migrating through electrolyte saturated sand columns are reported in Figure 2.1b. Interestingly, the results observed for *Y. enterocolitica* show an opposite trend to those noted for *E. coli* O157:H7. Specifically, for *Y. enterocolitica*, the average attachment efficiency is greater when the cells are grown in the absence of oxygen ( $\alpha_{\text{avg}} \approx 0.44$ ) in comparison to when they are grown under aerobic conditions ( $\alpha_{\text{avg}} \approx 0.20$ ). A previous study examining the adhesion of strictly anaerobic bacteria onto glass coverslips under anaerobic and aerobic incubation

periods demonstrated similar behavior (26). Specifically, it was shown that incubation in the presence of air significantly decreased adhesion of *Syntrophomonas wolfei* and *Desulfovibrio sp.* strain G11 onto glass in comparison to completely anaerobic incubation (26). Hence, our results and those of previous studies show that our understanding of the influence of oxygen tension during growth on bacterial transport is still too limited to allow generalization. Further studies examining the influence of this environmental parameter on the migration behavior of a broader selection of organisms are needed. The causes of the bacterial deposition behavior observed in Figure 2.1 will be discussed in more detail later in the paper.

### **2.4.3 Effect of Oxygen Tension during Acclimatization on Bacterial Transport in Packed Column**

In this section, we examine the effect of DO concentration during cell acclimation on the transport and deposition behavior of the two selected pathogenic bacteria. For both *E. coli* and *Y. enterocolitica*, the attachment efficiency is not affected by the DO content of the acclimation solution when they are grown aerobically (at a 95% confidence level) (Figure 1). For instance, in the case of *E. coli*,  $\alpha \approx 0.90$  when the cells are acclimated in either lowDO (AERlow) or satDO (AERsat) electrolyte solutions (Figure 2.1a). Similarly, for *Y. enterocolitica*,  $\alpha$  is 0.20 whether the organism is acclimated in lowDO (AERlow) or satDO (AERsat) electrolyte (Figure 2.1b). In contrast, the bacterial deposition behavior is affected by the DO concentration during acclimation when cells are grown under anaerobic conditions. *E. coli* O157:H7 experiences an increase in  $\alpha$  (from 0.47 to 0.70) when suspended in electrolyte that is saturated with oxygen (ANAsat) (Figure 1a). Here again, *Y. enterocolitica* shows a behavior that is opposite to that observed for *E. coli* O157:H7. Namely, when cells are grown anaerobically, this

organism exhibits a decrease in  $\alpha$  (from 0.60 to 0.28) when acclimated in electrolyte that is oxygen rich (ANAsat) in contrast to electrolyte that is oxygen deficient (ANALow) (Figure 2.1b). These data suggest that the effect of oxygen tension during cell acclimation on bacterial transport and deposition in granular porous media cannot yet be readily generalized. The results shown in Figure 2.1 are particularly interesting as they highlight the importance of cell type (and respective surface characteristics) in the potential influence of this environmental parameter on bacterial adhesion.

#### **2.4.4 Linking Bacterial Transport Behaviour to Cell Properties**

The image analysis data presented in Figure 2.2 clearly demonstrates that both *E. coli* O157:H7 and *Y. enterocolitica* are rod shaped organisms, with *Y. enterocolitica* being more elongated. Others have shown that rod shaped particles and more elongated bacteria are retained more readily in granular porous media than spherical colloids (19, 20). However, inspection of the data in Figures 2.1 and 2.2 does not reveal greater retention of bacteria with higher aspect ratios. Furthermore, the results do not show increased retention of larger cells as may be expected if physical straining were an important mechanism (27). In fact, the data in Figures 2.1 and 2.2 shows that the larger cells (*Y. enterocolitica*) generally exhibit lower retention rates than the smaller cells (*E. coli*). Hence, a physical retention mechanism is likely not controlling the extent of bacterial migration in this system.

In Figure 2.1, the bacterial cell EPM (scatter plot) is presented on the same graph as the measured attachment efficiency (bar plot). For *E. coli* O157:H7, the trend in  $\alpha$  from the leftmost treatment to the rightmost treatment follows the same trend as the EPM (Figure 2.1a). Specifically, the conditions with the highest attachment efficiency (AER)

exhibit the lowest absolute charge. In a similar manner, the condition with the lowest  $\alpha$  value is linked with the greatest absolute charge (ANALow). A simple linear regression of  $\alpha$  against EPM for *E. coli* O157:H7 (that includes all four treatments) reveals a significant correlation in the two sets of measurements ( $R^2=0.98$ , with a slope of 2.5). Such direct links between cell surface charge (e.g., EPM or zeta potential) and bacterial transport in granular porous media have previously been shown by several researchers (6, 28, 29). Indeed, these results are generally in qualitative agreement with the classical Derjaguin-Landau-Verwey-Overbeek (DLVO) theory of colloidal stability for the interaction of a negatively charged particle (i.e., the bacterial cell) with a negatively charged surface (i.e., the quartz sand surface) (30, 31). According to this theory, cells with a lower absolute potential (or EPM) will experience a lower repulsive force as they approach the sand grain surface (assuming all other properties remain constant). The data shown in Figure 2.1a suggests that cell EPM (or zeta potential) is the key factor controlling the transport and deposition behavior of *E. coli* O157:H7 when grown or acclimated at two different DO levels.

Measured EPMs and attachment efficiencies for *Y. enterocolitica* are plotted together in Figure 2.1b. Although not as strong as in the case of *E. coli*, the trend in EPM is generally in agreement with the observed changes in  $\alpha$  values. For instance, the conditions with the lowest attachment efficiency (aerobic growth) are associated with the greatest absolute charge (at a 95% confidence level), demonstrating qualitative agreement with DLVO theory. A linear regression of  $\alpha$  against EPM for *Yersinia* (including four treatments) reveals a weaker correlation in the two sets of measurements ( $R^2=0.68$ ) but, interestingly, with a comparable slope (2.4) to that observed for *E. coli* (2.5).

Lower  $\alpha$  values are generally measured with *Yersinia* in comparison to *E. coli* (with the exception of the ANA<sub>low</sub> condition). This trend in the behavior of the two organisms is also in qualitative agreement with DLVO theory because the absolute EPM of *Yersinia* is nearly 10 times greater than that of *E. coli* O157:H7. Generally, the data shown in Figure 2.1 demonstrate that DLVO interactions control the migration of the two cell types when grown or acclimated at different oxygen tensions. However, it should be noted that the ANA<sub>low</sub> treatment for *Yersinia* exhibits non-DLVO behavior. Specifically, even though this condition is linked with a relatively high attachment efficiency (~0.6) which is comparable to the  $\alpha$  value measured for *E. coli* for the ANA<sub>sat</sub> condition (~0.7), the absolute charge of *Yersinia* (absolute EPM of 1.3  $\mu\text{mcm/Vsec}$ ) is much greater than that measured for *E. coli* (absolute EPM of 0.18  $\mu\text{mcm/Vsec}$  for ANA<sub>sat</sub>). Clearly, a number of non-DLVO interactions could also contribute to the observed transport and deposition behavior of *Yersinia* in this study; including, but not limited to, electrosteric interactions and Lewis acid-base interactions (32).

## 2.5 Environmental Implications

This study highlights the variability in bacterial cell surface properties and deposition behavior in granular porous media as a result of changes in water oxygen tension that may occur during cell growth or acclimation. To our knowledge, a well-controlled laboratory investigation of the effect of oxygen tension during growth and acclimation of waterborne bacterial pathogens on their migration behavior in granular porous media has not been previously reported. Our results show how the influence of DO on bacterial transport and deposition is strongly dependent on the species examined. Significantly different results were obtained when experiments were conducted with *E. coli* O157:H7

or *Y. enterocolitica*. For instance, *E. coli* exhibits the least extent of migration when grown aerobically, whereas *Yersinia* exhibits the greatest migration potential when grown in the presence of O<sub>2</sub>. Such variations in bacterial transport behavior may have important implications for predictions of groundwater contamination potential or of pathogen removal efficiencies in engineered water treatment facilities.

Our study also reveals significant variations in cell surface charge (measured by potentiometric titration), electrophoretic mobility, and cell size and shape when DO concentrations are changed during bacterial growth or acclimation. It should be noted that potentiometric titrations alone cannot be used to conclusively determine the types of dissociable functional groups or biomolecules present on the bacterial cell surface. A better understanding of the composition of the outer cell membrane can be obtained by coupling potentiometric titrations with another characterization technique (e.g., ATR-FTIR). Ongoing research in our laboratory is aimed at improving our understanding of the influence of DO on the composition of the bacterial cell membrane using this technique. As evidenced by this investigation, an improved characterization of the bacterial cell wall will lead to a better understanding of bacteria-surface interactions in a broad range of environmentally relevant applications.

In this work, we have focused on the influence of extremes in DO levels during bacterial growth and acclimation on bacterial migration and cell surface properties. Bacterial transport and deposition was examined at two DO levels (high and low) using columns packed with clean high-purity quartz sand. However, in natural and engineered granular matrices, variations in DO concentration can also influence the chemical composition of granular collector surfaces. For instance, in shallow groundwater aquifers, aerobic conditions can lead to the formation of metal (e.g., iron or manganese)

oxides on the surface of soil grains that give rise to important charge heterogeneities. Such “patches” of surface charge heterogeneity have previously been shown to control particle-surface or microbe-surface interactions (33). Yet, additional studies are needed to better understand the potential competing or synergetic effects of varying DO levels during bacterial growth, acclimation and transport in geochemically heterogeneous systems.

## **2.6 Acknowledgements**

This research was supported by the Fonds québécois de la recherche sur la nature et les technologies (FQRNT Team Grant), the Centre for Host-Parasite Interactions at McGill (New Initiatives Grant), the Canadian Water Network (CWN) and the Canada Foundation for Innovation (CFI). The authors acknowledge G. Faubert (McGill) and C. Madramootoo (McGill) for helpful discussions, S. Gruenheid (McGill) for providing ATCC 700927 and M. Assanta (AAFC) for providing ATCC 23715.

## 2.7 Literature Cited

1. Steffan, R. J.; Sperry, K. L.; Walsh, M. T.; Vainberg, S.; Condee, C. W., Field-scale evaluation of in situ bioaugmentation for remediation of chlorinated solvents in groundwater. *Environ. Sci. Technol.* **1999**, *33*, 2771-2781.
2. Tufenkji, N.; Ryan, J. N.; Elimelech, M., The promise of bank filtration. *Environ. Sci. Technol.* **2002**, *36*, (21), 422a-428a.
3. Emelko, M. B., Removal of viable and inactivated *Cryptosporidium* by dual- and tri-media filtration. *Water Res.* **2003**, *37*, 2998-3008.
4. Harvey, R. W.; Harms, H., Transport of microorganisms in the terrestrial subsurface: In situ and laboratory methods. In *Manual of Environmental Microbiology*, 2nd ed.; Hurst, C. J., Ed. ASM Press: Washington, D.C., 2001; pp 753-776.
5. Tufenkji, N., Modeling microbial transport in porous media: Traditional approaches and recent developments. *Adv. Water Resour.* **2007**, *30*, 1455-1469.
6. Castro, F. D.; Tufenkji, N., Relevance of nontoxigenic strains as surrogates for *E. coli* O157:H7 in groundwater contamination potential: role of temperature and cell acclimation time. *Environ. Sci. Technol.* **2007**, *41*, 4332-4338.
7. Harter, T.; Wagner, S.; Atwill, E. R., Colloid transport and filtration of *Cryptosporidium parvum* in sandy soils and aquifer sediments. *Environ. Sci. Technol.* **2000**, *34*, (1), 62-70.
8. Valett, H. M.; Morrice, J. A.; Dahm, C. N.; Campana, M. E., Parent lithology, surface-groundwater exchange, and nitrate retention in headwater streams. *Limnol. & Oceanography* **1996**, *41*, (2), 333-345.
9. Goldscheider, N.; Hunkeler, D.; Rossi, P., Review: Microbial biocenoses in pristine aquifers and an assessment of investigative methods. *Hydrogeology J.* **2006**, *14*, 926-941.
10. Datry, T.; Malard, F.; Gibert, J., Dynamics of solutes and dissolved oxygen in shallow urban groundwater below a stormwater infiltration basin. *Sci. Total Environ.* **2004**, *329*, 215-229.

11. Sharma, P. K.; McInerney, M. J.; Knapp, R. M., In situ growth and activity and modes of penetration of *Escherichia coli* in unconsolidated porous materials. *Appl. Environ. Microbiol.* **1993**, *59*, (11), 3686-3694.
12. Reynolds, P. J.; Sharma, P. K.; Jenneman, G. E.; McInerney, M. J., Mechanisms of microbial movement in subsurface materials. *Appl. Environ. Microbiol.* **1989**, *55*, (9), 2280-2286.
13. Yang, H.-H. The effect of environmental stress on cell surface properties and their relation to microbial adhesion in feedlot *Escherichia coli* isolates. Ph.D., University of Connecticut, 2005.
14. Yang, H.-H.; Morrow, J. B.; Grasso, D.; Vinopal, R. T.; Smets, B. F., Intestinal versus external growth conditions change the surficial properties in a collection of environmental *Escherichia coli* isolates. *Environ. Sci. Technol.* **2006**, *40*, 6976-6982.
15. Landini, P.; Zehnder, A. J. B., The global regulatory *hns* gene negatively affects adhesion to solid surfaces by anaerobically grown *Escherichia coli* by modulating expression of flagellar genes and lipopolysaccharide production. *Appl. Environ. Microbiol.* **2002**, *184*, (6), 1522-1529.
16. Tufenkji, N.; Elimelech, M., Correlation equation for predicting single-collector efficiency in physicochemical filtration in saturated porous media. *Environ. Sci. Technol.* **2004**, *38*, 529-536.
17. Arneborg, N.; Salskov-Iversen, A. S.; Mathiasen, T. E., The effect of growth rate and other growth conditions on the lipid composition of *Escherichia coli*. *Appl. Microbiol. Biotechnol.* **1993**, *39*, (3), 353-357.
18. Tang, Y.; Hollingsworth, R. I., Regulation of lipid synthesis in *Bradyrhizobium japonicum*: low oxygen concentrations trigger phosphatidylinositol biosynthesis. *Appl. Environ. Microbiol.* **1998**, *64*, (5), 1963-1966.
19. Weiss, T. H.; Mills, A. L.; Hornberger, G. M.; Herman, J. S., Effect of bacterial cell shape on transport of bacteria in porous media. *Environ. Sci. Technol.* **1995**, *29*, 1737-1740.
20. Salerno, M. B.; Flamm, M.; Logan, B. E.; Velegol, D., Transport of rodlike colloids through packed beds. *Environ. Sci. Technol.* **2006**, *40*, 6336-6340.

21. Haas, J. R., Effects of cultivation conditions on acid–base titration properties of *Shewanella putrefaciens*. *Chemical Geol.* **2004**, *209*, 67-81.
22. De Leon, A.; Hernandez, V.; Galindo, E.; Ramirez, O. T., Effects of dissolved oxygen tension on the production of recombinant penicillin acylase in *Escherichia coli*. *Enz. Microbial Technol.* **2003**, *33*, 689-697.
23. Pederson, K. J.; Pierson, D. E., Ail expression in *Yersinia enterocolitica* is affected by oxygen tension. *Infect. Immunity* **1995**, *63*, (10), 4199-4201.
24. Salmon, K. A.; Hung, S.; Steffen, N. R.; Krupp, R.; Baldi, P.; Hatfield, G. W.; Gunsalus, R. P., Global Gene Expression Profiling in *Escherichia coli* K12: Effects of oxygen availability and ArcA. *J. Biological Chem.* **2005**, *280*, (15), 15084-15096.
25. Colon-Gonzalez, M.; Mendez-Ortiz, M. M.; Membrillo-Hernandez, J., Anaerobic growth does not support biofilm formation in *Escherichia coli* K-12. *Res. in Microbiol.* **2004**, *155*, 514-521.
26. van Schie, P. M.; Fletcher, M., Adhesion of biodegradative anaerobic bacteria to solid surfaces. *Appl. Environ. Microbiol.* **1999**, *65*, (11), 5082-5088.
27. Bradford, S. A.; Yates, S. R.; Bettahar, M.; Simunek, J., Physical factors affecting the transport and fate of colloids in saturated porous media. *Water Resour. Res.* **2002**, *38*, (12), 1327-1338.
28. Redman, J. A.; Walker, S. L.; Elimelech, M., Bacterial adhesion and transport in porous media: role of the secondary energy minimum. *Environ. Sci. Technol.* **2004**, *38*, 1777-1785.
29. Bolster, C. H.; Walker, S. L.; Cook, K. L., Comparison of *Escherichia coli* and *Campylobacter jejuni* transport in saturated porous media. *J. Environ. Qual.* **2006**, *35*, 1018-1025.
30. Derjaguin, B. V.; Landau, L. D., Theory of the stability of strongly charged lyophobic sols and of the adhesion of strongly charged particles in solutions of electrolytes. *Acta Physicochim. URSS* **1941**, *14*, 733-762.
31. Verwey, E. J. W.; Overbeek, J. T. G., Theory of the stability of lyophobic colloids. Elsevier: Amsterdam, 1948.
32. Van Oss, C. J., *Interfacial Forces in Aqueous Media*. 2nd ed.; CRC Press: 2006.

33. Abudalo, R. A.; Bogatsu, Y. G.; Ryan, J. N.; Harvey, R. W.; Metge, D. W.; Elimelech, M., Effect of ferric oxyhydroxide grain coatings on the transport of bacteriophage PRD1 and *Cryptosporidium parvum* oocysts in saturated porous media. *Environ. Sci. Technol.* **2005**, *39*, 6412-6419.

## CHAPTER 3

### Effect of Dissolved Oxygen on the Physicochemical Properties of Selected Pathogenic Bacteria

#### 3.1 Abstract

The main objective of this study is to investigate at the molecular level the bacterial cell surface in order to better understand the factors that conferred to *Escherichia coli* O157:H7 and *Yersinia enterocolitica* their observed adhesive behavior in Chapter 2. The goal is to investigate the relationship of the outer membrane physicochemical properties on environmental factors such as the antecedent growth condition and the dissolved oxygen during acclimation for these two bacterial pathogens. Experiments were conducted to evaluate the variations in cell wall chemistry in terms of the identity and abundance of cell surface functional groups as a function of environmental DO concentration during growth and acclimatization. Macroscopic methods such as titration of bacterial cells coupled with previous zeta potential data, along with the modeling of the experimental data are utilized to find the major proton-active functional groups and the overall cell surface charge at the cell membrane. ATR-FTIR spectroscopy was used to examine the interfacial properties of the cells in order to reveal and characterize the active functional groups and macromolecular structures that might be involved in the development of the charge of the pathogens studied. Results of the integrated carbohydrate IR zone, showed a clear difference between growth protocols and their association with general molecular composition of the bacterial membrane. Titration of cells showed an overall association between charge by zeta potential and concentration of cell surface functional groups as a function of the growth protocol. In this work, the

antecedent growth protocol has been found to modify the properties of the outer surface wall of the two bacterial pathogens explaining most of the behavior seen previously in Chapter 2. Results also allowed to hypothesize about molecular elements such as LPS likely associated with the non-DLVO behavior.

### **3.2 Introduction**

Naturally occurring environmental processes such as bacterial transport in the natural subsurface environment, the onset of biofilm formation in water distribution systems, and retention of bacteria in engineered water treatment systems are all dependent on the complex interplay of fundamental interactions controlling bacterial adhesion to inert surfaces [1-3]. Most bacteria-surface interactions are believed to be mediated by the outer membrane of bacterial cells. Previous studies have demonstrated that bacteria growth conditions can influence the density and distribution of cell surface functional groups on Gram-positive [4, 5] and Gram-negative [6-11] bacterial surfaces. Accordingly, bacteria-surface interactions may be affected by variations in the composition of the outer membrane of bacterial cells with changes in environmental conditions (e.g., pH, temperature, substrate availability and composition)[9, 11, 13, 14, 22, 25, 36]. Nevertheless, the ability of bacteria, and more specifically pathogens, to interact with and attach to surfaces under different environmental conditions is to date not very well understood [2, 12-16].

Bacterial cell walls consist of a wide range of biopolymers and macromolecules, which possess carboxyl, hydroxyl, phosphate, and amide functional groups that confer to the cells a net charge. In many aquatic environmental systems, this net charge is determined to be negative [15, 17, 18]. Recent metal adsorption studies indicate the

important role of acidic ligands such as carboxyl or phosphate on proton-exchange processes involving electrostatic interactions [4, 5, 19]. The relative abundance of certain proton-active surface ligands arising from cell wall macromolecules, such as teichoic and teichuronic acids in the case of Gram-positive cells and lipopolysaccharides (LPS) in the case of Gram-negative cells, has been shown to influence the metal sorption process [4, 20, 21] and the extent of electrostatic interactions between bacteria and silica surfaces [11, 22]

Macroscopic acid-base titration has been used increasingly over the last decade to yield practical information about the concentration and acidity of proton-active surface ligands, [6, 7, 19, 23, 26]. Nevertheless, this technique alone does not provide sufficient information to establish the identity of reactive surface ligands [16]. Recent studies indicate that spectroscopic techniques may be useful complementary tools to study the molecular-scale processes that govern proton-bacteria sorption reactions [9,4]. Infrared (IR) spectroscopy is a well-established analytical technique that can be used to determine the identity and protonation states of organic functional groups [27,28]. Proteins, lipids and carbohydrates have been widely investigated individually and, more recently, this technique has been applied to more complex systems [12, 29, 30]. Because IR radiation is nondestructive to biological materials, it can be used to examine the functional group chemistry of living cells and isolated cellular components [12, 20, 27, 29]. As a result, IR spectroscopy has been utilized for *in situ* examination of bacterial cells, biofilms and extracted bacterial surface biomolecules in aqueous systems [12, 29, 30, 34]. Several recent investigations have examined the surface chemistry of intact bacterial cells and their cell walls using both macroscopic (e.g., potentiometric titration, ion adsorption) and molecular tools (e.g. FTIR and XPS) [11, 12, 20, 31, 33]. By combining IR data with

information regarding the  $pK_a$  values of acid/base functional groups in the cell surface, tentative identifications of the functional groups associated with the  $pK_a$  values derived from potentiometric data can be made.

Changes in the expression of nutrient-specific binding agents and membrane transport proteins, lipopolysaccharides, flagella, etc. have been demonstrated to occur upon switching between metabolic pathways and can therefore alter the ability of microbes to stick to surfaces [35, 36]. Eboigbodin [11] reported that the surface chemistry of *E. coli* was altered after supplementation of the growth medium with additional glucose at the beginning of the growth phase. Specifically, results obtained using potentiometric titrations and spectroscopic techniques, showed that cells displayed a higher concentration of proton-active functional groups from macromolecules present at the cell surface that consequently reduced cell-to-cell aggregation. Haas [7] found sufficient variability by potentiometric titration of the facultative *Shewanella putrefaciens*, when culture conditions were changed from aerobic to anaerobic, as to confirm two distinct sets of surface complexation parameters. On the other hand, in a study of *Bacillus* and *Pseudomonas* spp. by ATR-FTIR spectroscopy, Jiang *et al* reported that bacterial surface chemistry did not change significantly with either the growth phase or the composition of the nutrient-rich growth media [12]. Clearly, discrepancies remain regarding metabolic determinants of microbial surface reactivity.

In the present study, experiments were conducted to evaluate the variations in cell wall chemistry in terms of the identity and abundance of cell surface functional groups as a function of environmental dissolved oxygen (DO) concentration during growth and acclimatization of *Escherichia coli* O157:H7 and *Yersinia enterocolitica*. These bacterial pathogens, which are both facultative anaerobes, are able to grow in a wide range of

environments, and hence investigating the dependence of their physicochemical properties on environmental factors is of paramount importance. Furthermore, following exposure to different environmental settings readily found in the natural subsurface [37,38], changes in the mobility of these pathogens mediated by intrinsic outer membrane properties can lead to contamination of potable water supplies due to increased migration potentials. In this work, macroscopic methods, such as titration of bacterial cells, along with the modeling of the experimental data were utilized to identify the major proton-active functional groups and the overall cell surface charge at the cell membrane. ATR-FTIR spectroscopy was then used to characterize the proton-active functional groups and macromolecular structures that might be involved in the development of the charge of the pathogens studied.

### **3.3 Materials and Methods**

#### **3.3.1 Experimental Design**

Four treatments were considered, aiming to investigate the influence of oxygen tension (DO) during bacteria growth and acclimatization on bacterial surface properties. Selected bacteria were grown either anaerobically (ANA) or aerobically (AER), then resuspended in a prepared electrolyte solution (10 mM KCl) of either low dissolved oxygen (lowDO) or saturated DO (satDO) concentration. Following a 21 h acclimation period in the lowDO or satDO electrolyte solution at 9 °C, bacteria titrations (11 °C) and FTIR experiments were conducted.

#### **3.3.2 Bacteria Selection and Growth Protocols**

Two pathogenic microorganisms were selected for this study, *Escherichia coli* O157:H7 ATCC 700927 and *Yersinia enterocolitica* ATCC 23715. Pure cultures were maintained

at  $-80\text{ }^{\circ}\text{C}$  in Luria-Bertani Lennox broth (20 g/L, Fisher) with 15% glycerol. One day prior to inoculation, frozen cultures were streaked onto solid LB agar plates that were then incubated at  $37\text{ }^{\circ}\text{C}$  for 21 h. For each experiment, a scrape from the starter plate was used to inoculate sterile LB broth. Aerobic (AER) growth for both strains involved incubation at  $37\text{ }^{\circ}\text{C}$  and 200 rpm for 8 h in 150 mL of LB broth (in a 500 mL baffled flask), at which point the cells were harvested. Anaerobic (ANA) growth for both strains involved incubation at  $37\text{ }^{\circ}\text{C}$  in 200 mL of LB broth in capped 250 mL centrifuge tubes (PPCO, Nalgene) maintained without agitation for 20 h.

### **3.3.3 Bacteria Acclimation Protocol**

Following the selected growth protocol (AER or ANA), the bacteria culture was centrifuged (Sorvall RC6) for 15 min at 5860 g in an SS-34 rotor (Kendro). The growth medium was decanted and the pellet was resuspended in freshly prepared electrolyte (either lowDO or satDO 10 mM KCl solution). To remove all traces of the growth medium, the cells were centrifuged and resuspended in fresh electrolyte one additional time. Analytical reagent grade KCl,  $\text{KHCO}_3$ , KOH and HCl (Fisher) and deionized (Milli-Q) water (DI) were used to prepare all electrolyte solutions. The satDO electrolyte was prepared by vigorous stirring and sparging of 1.2 L KCl solution (10 mM) using filtered (Durapore PVDF membrane, 0.22  $\mu\text{m}$ , Millipore) air at 1.8 vvm in a 2 L Erlenmeyer flask for 30 min. The final DO level of the satDO solution was  $8.6\pm 0.3$  mg DO/L. The lowDO electrolyte was prepared by vigorously stirring and sparging a 1.2 L KCl solution (10 mM) with prepurified  $\text{N}_2$  at 1.8 vvm in a tightly capped 2 L Erlenmeyer flask for 30 min. The final DO level of the lowDO electrolyte was  $0.4\pm 0.3$  mg DO/L. Prepared lowDO or satDO electrolytes were transferred to a 2 L low gas permeability

bioprocess bag (Labtainer, Hyclone) using a glass tube positioned at the bottom of the 2 L flask while keeping a positive N<sub>2</sub> pressure. After transfer of the lowDO or satDO electrolytes to the Labtainer bag, the total equivalent dissolved CO<sub>2</sub> concentration was adjusted to  $\sim 1.2 \times 10^{-5}$  M using 0.1M KHCO<sub>3</sub> (Fisher) and the pH was adjusted to 6.7±0.2 using 0.1 M HCl or 0.1M KOH (Fisher). Washed cells were resuspended to a final concentration of  $\sim 4 \times 10^7$  cells/mL in either lowDO or satDO electrolyte contained in a separate 500 mL Labtainer bag. The Labtainer bags holding the bacteria suspension were then maintained at 9°C for 21 h. This cold temperature acclimatization was used to replicate conditions that may be encountered by cells following release into groundwater representative of the Canadian climate. Actual DO levels of the background solution and bacteria suspension were verified using a micro flow-through polarographic DO probe (Model DO-166FT, Lazar Labs, US) connected to the Labtainer bag.

### **3.3.4 ATR-FTIR Spectroscopy**

ATR-FTIR spectra were recorded on a Varian Excalibur 3100 FTIR spectrometer (Varian, Melbourne, Australia) equipped with a DTGS detector and a SensiIR single-bounce ATR accessory with a ZnSe/diamond crystal (Smith Scientific, CT). The instrument was purged with dry air to minimize spectral contributions from CO<sub>2</sub> and water vapor. For each of the four treatments examined, after acclimatization ( $4 \times 10^7$  cells/mL), washed cell suspensions were immediately concentrated by centrifugation to  $\sim 5 \times 10^9$  cells/mL. Subsequently, cell suspensions with pH values of 4.0, 6.7 and 9.5 were prepared separately by adding appropriate quantities of 0.1 M HCl or 0.1 M NaOH. Next, for each treatment, a 1.5 mL sample of the bacterial suspension was spun down into a pellet (9000g for 4 min, microCL 17R, ThermoE), which was then carefully placed onto

the clean ATR crystal. The ATR-FTIR spectrum of the wet pellet paste was acquired by co-addition of 100 scans with a resolution of  $4\text{ cm}^{-1}$  and ratioed against a background spectrum previously collected from the clean ATR crystal. For all four experimental treatments, a reference spectrum of preconditioned 10 mM KCl water solution was subtracted from the spectrum of each bacterial sample, with the subtraction scaling factor set such as to obtain an absorbance ratio of the amide I to the amide II band of  $1.4 \pm 0.02$ . The resulting spectrum was then normalized to unit height of the amide I band.

### 3.3.5 Bacterial Cell Characterization

Microelectrophoresis (ZetaSizer Nano ZS, Malvern) was used to characterize the electrokinetic properties of the cells. Electrophoretic mobility (EPM) was measured at 11 °C using cell suspensions ( $\sim 4 \times 10^7$  cells/mL) prepared at treatment of interest. These measurements were repeated using at least three different fresh bacterial suspension samples, measured at least three times each.

Bacterial cell concentrations and standard curves were determined with a Helber bacteria counting chamber (SV400, Proscitech) by analyzing images taken in an inverted microscope (IX-71, Olympus) operating in phase contrast mode.

### 3.3.6 Titrations of Bacteria Cells

Potentiometric titrations were conducted to determine the deprotonation constant values ( $pK_a$ ) and proton binding site concentrations ( $S_i$ ) of acid/base functional groups located in the macromolecules forming the bacterial outer cell wall. Bacterial suspensions grown under the four previously described treatment protocols were resuspended in 10 mM KCl to a concentration of  $7.5 \times 10^9$ — $1.1 \times 10^{10}$  cells/mL and stored at 9 °C inside Labtainer

bags. After 21 h of acclimation, 50 mL of the bacterial suspensions were purged for 20 min with N<sub>2</sub> gas in a glass jacketed vessel which kept contents at 11 °C. Before each experiment, aliquots of the bacteria suspension were used to determine the cell concentration. Cells suspensions provided enough buffering capacity to warrant at least 4 times more base compared to the blank titrations. Titrations were repeated at least twice in the pH range of 3.4 to 11.0 at 11±0.3 °C using a 798 Titrino automatic titrator (Metrohm Ltd.) under a N<sub>2</sub> atmosphere. At each titration step, a stability of 0.1 mV/s was reached before the next aliquot of titrant was added. The titrant solution (0.1 N NaOH) was degassed for 30 min prior to titrations. Standardized degassed 0.1 N HCl was used to bring the initial suspension pH to 3.4. The charge excess per cell, [H<sup>+</sup>]<sub>ex</sub>, (mmol/10<sup>8</sup> cells) was calculated from the titration measurements as follows [4]:

$$[\text{H}^+]_{\text{ex}} = (C_A - C_B - [\text{H}^+] + K_w/[\text{H}^+]) / N_{\text{bact}} \quad (1)$$

where  $N_{\text{bact}}$  is the total number of bacterial cells per mL of solution,  $C_A$  and  $C_B$  are concentrations of acid and base added,  $[\text{H}^+]$  is obtained from the measured pH, and  $K_w$  is the stability constant for the dissociation of water. The  $\text{p}K_a$  values of ionizable functional groups on the cell surface and corresponding concentrations of these groups ( $S_i$ ) were evaluated using the chemical speciation software FITEQL 4.0 as previously shown [10, 13, 39]. Titrations conducted on blank (bacteria-free) solutions of low or saturated DO were used to normalize the raw data obtained from titrations of bacterial suspensions. It has been previously demonstrated in the literature that a non-electrostatic model (NEM) in FITEQL provides good fitting to experimental bacterial titration data [8, 10, 13, 19]. In this study, best fits of the NEM to the experimental data were obtained while using four and three proton binding sites for *E. coli* and *Y. enterocolitica*, respectively.

Data obtained from potentiometric titrations were modeled using the FITEQL 4.0 optimization routine [39] to determine the intrinsic deprotonation constants ( $pK_a$ ), surface site densities ( $S_i$ ), and deprotonation profiles of chemical species as a function of pH. The fit of the experimental data with the surface complexation model intrinsically presumes that the observed buffering is due to the deprotonation of functional groups (e.g., carboxyl, phosphate, hydroxyl, amine, etc.) in the cell wall. FITEQL 4.0 fits the experimental data to a specified model (in this case, the non electrical double layer model) by calculating the variance,  $V(Y)$  between the experimental data and the model:

$$V(Y) = \frac{\sum \left( \frac{Y_{calc} - Y_{obs}}{S_{obs}} \right)^2}{n_p n_{II} - n_u} \quad (2)$$

where  $Y_{calc}$  is the calculated value,  $Y_{obs}$  is the experimental value,  $S_{obs}$  is the error associated with the experimental data,  $n_p$  is the number of data points,  $n_u$  is the number of adjustable parameters in the model and  $n_{II}$  is the number of so-called Group II components, for which both the total and free (dissolved) concentrations are known. Thus, the variance is a quantitative estimate of the success with which the specified model describes the data such that  $0.1 \leq V(Y) \leq 20$  is considered a good fit [39]. It follows from equation 2 that as the number of adjustable parameters increases (e.g., by adding more proton binding sites to the surface), the variance should increase, unless the model with more parameters provides a better description of the data. Thus, potentiometric titrations were fit with a model in which the number of functional groups present on the bacterial surface was varied, with two adjustable parameters; namely the value of the deprotonation constants ( $pK_a$ ) and total site density. This computational

approach has been previously used to determine  $pK_a$  values and their corresponding site concentrations on bacterial cell surfaces [9, 10, 13, 19, 26].

The outer cell membrane may display several different functional groups, assigned as  $L_1, L_2 \dots L_n$  (where  $L_iH$  corresponds to the protonated species). The deprotonation of the functional group  $L_iH$  can be expressed by the following chemical reaction and mass balance.



$$K_i = \frac{[RL_i^-]a_{H^+}}{[RL_iH^0]} \quad (4)$$

where  $R$  represents the cell surface molecule to which the acid/base functional group is attached,  $K_i$  represents the deprotonation stability constant, and  $a$  represents the activity of the subscripted species. The  $pK_a$  values, where  $pK_a = -\log(K_a)$ , and their corresponding site concentrations can be characterized directly from the acid–base titration data.

### 3.4 Results and Discussion

#### 3.4.1 Electrokinetic Characterization of Bacteria

Several studies on the transport and fate of colloids and biocolloids have demonstrated the relevance of zeta potential as a predictor of particle stability and interaction potential with abiotic surfaces [1, 3, 15, 45, 46]. Bacteria  $\zeta$ -potentials were calculated from EPM measurements previously reported in Chapter 2. Both *E. coli* and *Y. enterocolitica* exhibit a net negative charge at pH 6.7 (Figure 3.1). However, there is a considerable difference in the charge of the two organisms over the range of treatments considered. *Y. enterocolitica* has a substantially more negative  $\zeta$ -potential than *E. coli* (ranging from 5 to

15 times larger depending on the treatment). The data in Figure 3.1 shows that *E. coli* exhibits a more negative overall charge for the anaerobic growth treatments, with the ANA<sub>low</sub> condition being most negatively charged. This latter result suggests that the DO concentration during acclimatization influences the overall cell surface charge. *Y. enterocolitica* exhibits an opposite trend whereby cells grown aerobically are slightly ( $p < 0.01$ ) more charged than those grown anaerobically (Figure 3.1). Roberts et al. [47] reported a similar trend with the organism *Shewanella putrefaciens* whereby aerobically grown cells were slightly more negative than anaerobically grown cells between pH 2–4.

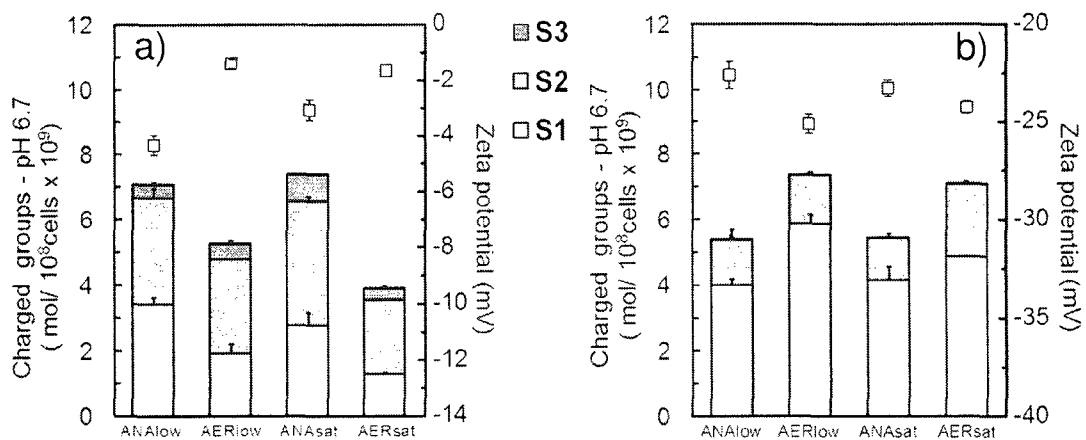


**FIGURE 3.1** Concentration of titrated charged sites at pH 6.7 following the four treatments for (a) *E. coli* O157:H7 and (b) *Y. enterocolitica* (bar graph). Scatter plots represent the zeta potential, where the error bars represent the 95% confidence interval.

### 3.4.2 Potentiometric Titrations

To better understand the nature of the functional groups present in the cell wall of the two organisms when grown and acclimatized at different DO concentrations, the data obtained from potentiometric titrations were analyzed using chemical speciation software (FITEQL 4.0). The  $pK_a$  values and concentrations of the proton binding sites determined

from this analysis are summarized in table 3.1. In general, the dissociation constants and site densities determined in this study are comparable to those determined in previous studies using other organisms [22, 31, 4, 5, 10]. The most acidic proton binding site determined for *E. coli* has  $pK_a$  values in the range of 3.4–4.1, coinciding with the  $pK_a$  range for phosphodiester (  $pK_1 = 3.4-4.1$ ) and falling within the  $pK_a$  range for carboxylic groups ( $pK_a = 2-6$ ) [24, 26, 33]. The second proton binding site for *E. coli*, with  $pK_a$  between 5.2 and 5.4, can be attributed to the carboxylic groups of organic acids, whereas the third  $pK_a$  (7.4–7.6) can be associated with phosphoryl groups [12, 42] and the most basic  $pK_a$  ( $\sim 10$ ) likely corresponds to either amine or hydroxyl (phenolic) groups. For *Y. enterocolitica*, FITEQL predicts three major proton binding sites and the fitted  $pK_a$ s can be tentatively assigned to carboxyl ( $pK_1$ ), phosphoryl ( $pK_2$ ), and amine/hydroxyl ( $pK_3$ ) groups. Predicted  $pK_a$  values for the two organisms for the four treatments are not very different (Table 3.1) suggesting that similar types of functional groups are present on both cell surfaces.

**TABLE 3.1:**  $pK_a$  values and their corresponding site concentrations ( $S_i$ ) for *E. coli* O157:H7 and *Y. enterocolitica*. Values in parentheses are one standard deviation of two experiments. Variance (goodness of fit) as calculated by FITEQL 4.0.

	Dissociation constants				Site concentration ( $10^9$ mol/ $10^8$ cells)					Variance
	$pK_1$	$pK_2$	$pK_3$	$pK_4$	$S_1$	$S_2$	$S_3$	$S_4$	$S_4^a$	$V(Y)$
<b><i>E. coli</i> O157:H7</b>										
ANA <sub>low</sub>	4.0 (0.2)	5.4 (0.2)	7.6 (0.1)	10.2 (0.0)	3.4 (0.2)	3.3 (0.4)	3.3 (0.3)	4.9 (0.3)	14.9 (0.6)	1.8
AER <sub>low</sub>	4.1 (0.1)	5.4 (0.1)	7.5 (0.0)	10.2 (0.2)	1.9 (0.2)	3.0 (0.0)	3.3 (0.2)	4.5 (0.2)	12.7 (0.3)	1.0
ANA <sub>sat</sub>	3.4 (0.3)	5.2 (0.0)	7.4 (0.0)	10.2 (0.0)	2.8 (0.3)	3.9 (0.1)	4.2 (0.0)	6.0 (0.2)	16.9 (0.4)	5.4
AER <sub>sat</sub>	3.6 (0.3)	5.4 (0.1)	7.5 (0.1)	10.3 (0.1)	1.3 (0.1)	2.4 (0.0)	2.5 (0.1)	3.2 (0.1)	9.4 (0.2)	2.6
<b><i>Yersinia enterocolitica</i></b>										
ANA <sub>low</sub>	4.9 (0.2)	7.0 (0.2)	10.0 (0.0)		4.0 (0.1)	2.8 (0.4)	5.5 (0.4)		12.3 (0.6)	11.6
AER <sub>low</sub>	4.5 (0.0)	7.2 (0.0)	10.1 (0.0)		5.9 (0.1)	5.1 (0.0)	9.3 (0.3)		20.3 (0.3)	15.5
ANA <sub>sat</sub>	4.8 (0.2)	6.8 (0.0)	9.9 (0.0)		4.2 (0.2)	3.4 (0.5)	6.8 (1.2)		14.4 (1.3)	13.3
AER <sub>sat</sub>	4.5 (0.1)	7.1 (0.0)	10.1 (0.0)		4.9 (0.3)	7.0 (0.0)	12.7 (0.1)		24.6 (0.3)	28.1

<sup>a</sup> Values in parentheses are one standard deviation of two experiments. Variance (goodness of fit) as calculated by FITEQL 4.0.

To allow comparison of the titration data with the  $\zeta$ -potential measurements, the concentration of deprotonated functional groups at the pH of interest (6.7) was determined. Specifically, the  $pK_a$  values determined by FITEQL were used to quantify the number of deprotonated groups at pH 6.7 for the four treatments. The contribution of each site to the total deprotonated charge at pH 6.7 is presented in Figure 3.1 for both bacteria. At pH 6.7, *E. coli* has a significantly larger amount of deprotonated sites (groups bearing a negative charge) per cell when grown anaerobically than when grown in the presence of oxygen at a 95% confidence level. At this pH, the number of charged groups in the ANALow condition is greater than in the AERsat condition. In contrast, it remains fairly constant in both ANALow and ANAsat treatments, suggesting little influence of the DO acclimatization treatment when *E. coli* is grown anaerobically. However, closer examination of Figure 3.1 shows that there is a difference in the relative contributions of the individual sites to the total charge, with the site  $S_1$  (tentatively assigned to phosphodiester groups) corresponding to nearly 50% of  $S_i$  in the ANALow, in comparison with 38% in the ANAsat condition. In contrast to the variability in  $S_1$ , the relative proportions of  $S_2$ ,  $S_3$  and  $S_4$  remain very similar throughout the four treatments. The site concentration at the most acidic site ( $pK_1$ ), greater in the ANALow condition than in the ANAsat condition in *E. coli* may provide insightful information for identification of key biomolecules that may be differentially expressed at the cell surface (e.g., LPS) as a response in DO changes during acclimation. This concept will be discussed in more detail later in the chapter.

Titration data presented in Figure 3.1 also provides insight on the surface charge of *Y. enterocolitica* at pH 6.7. In contrast to *E. coli*, *Y. enterocolitica* exhibits more

charged groups when grown aerobically than anaerobically and the number of charged groups for both growth conditions is not strongly dependent on the acclimatization protocol. Interestingly, the ANALow condition, which is one of the treatments exhibiting the lowest amount of proton binding sites ( $S_1$ ), in turn has the highest percentage of deprotonated groups per cell (48%), with  $S_1$  being the dominant charge-contributing group as seen in Figure 3.1. When grown aerobically, the average proportion of deprotonated groups to the total titrated charge per cell is about 32%. Haas reported similar behavior to that seen here with *Y. enterocolitica*; namely, *Shewanella putrefaciens* exhibited a greater number of charged sites when cells were grown aerobically [7].

Figure 3.1 allows for a direct comparison of  $\zeta$ -potential data with the number of charged groups at pH 6.7. For both organisms,  $\zeta$ -potential is generally well associated with the total concentration of charged functional groups at pH 6.7. Specifically, the treatments with the greatest amount of charged groups determined by titration analysis are generally associated with the highest absolute  $\zeta$ -potentials. Such direct links between cell  $\zeta$ -potential and titrated charge at a given pH have not been previously reported.

A simple linear regression of the total concentration of charged functional groups at pH 6.7 against  $\zeta$ -potential for *E. coli* O157:H7 considering all four treatments, reveals a rather weak correlation in the two sets of measurements with a  $R^2=0.66$ . Although, correlating only  $S_1$  (concentration of most acidic functional groups determined by the titration data analysis) and  $\zeta$ -potential the regression gives a  $R^2=0.87$  in which the relatively low concentration found at AERSat has a large influence in the correlation ( $R^2=0.999$  with all but the latter). In the case of *Y. enterocolitica* (Figure 3.1b) the trend in  $\zeta$ -potential is generally in better agreement with the observed changes in total charged functional groups at pH 6.7. A similar linear regression analysis on *Yersinia* (including

four treatments) reveals a correlation with an  $R^2=0.89$ , whereas correlating only  $S_1$  and  $\zeta$ -potential gives a correlation coefficient of  $R^2=0.94$ .

### **3.4.3 ATR-FTIR spectroscopy**

Characterization of bacterial outer membrane properties, such as the concentration of ionizable functional groups including carboxylic, phosphoric, phosphodiester, hydroxyl, and amine groups, is crucial for a better understanding of the factors controlling the development of cell surface charge. FTIR spectra of bacterial samples can provide insight into the biochemical composition of the cells, and when combined with  $pK_a$  analysis from titration measurements, provide a means to make tentative identifications of the functional groups responsible for the cell surface charge. In this study, we examine the potential of using ATR-FTIR spectroscopy to detect biochemical differences in the bacterial cell wall as a result of changes in available DO during cell growth and acclimatization.

The pH sensitivity of the intensities and band positions of the functional-group absorptions of cellular macromolecules was investigated by conducting ATR-FTIR measurements on samples prepared at three different pHs (4.8, 6.7, and 9.5). The assignment of the IR bands in the measured spectra to specific functional groups were based on band assignments previously reported for bacteria [12, 20, 27, 31, 48] and summarized in Table 3.2 with their corresponding frequencies.

**TABLE 3.2:** Functional groups and corresponding IR absorption frequencies encountered in both bacteria strains. Band assignment extracted from Naumann 2000, Dittrich and Sibley 2006 & 2005, Yee et al 2006 and Turney et al 2006.

Frequency (cm <sup>-1</sup> )	Functional group assignment
3000-2800	Stretching of C-H, -CH <sub>3</sub> , and >CH <sub>2</sub> functional groups
~1740	$\nu$ >C=O of ester functional groups primarily from membrane lipids and fatty acids
~1650	$\nu$ C=O of amides associated with proteins
~1595	$\delta$ O-H vibrations
~1540	$\delta$ N-H of amides associated with proteins
~1455	$\delta_{as}$ CH <sub>2</sub> / $\delta_{as}$ CH <sub>3</sub> of proteins
~1398	$\delta_{as}$ CH <sub>2</sub> / $\delta_{as}$ CH <sub>3</sub> and $\nu$ S-C-O of carboxylic groups
~1240	$\nu_{as}$ P=O of the phosphodiester backbone of nucleic acid and phospholipids
~1200-900	$\nu$ C-O-C of polysaccharides, ~1168, ~1110, 1050, 1030 for C-O
~1085	$\nu_{as}$ P=O of the phosphodiester backbone of nucleic acid (DNA and RNA)

$\nu_{as}$  = asymmetric stretching ;  $\nu_{s}$  = symmetric stretching;  $\delta$  = bending

In general, carboxylic acid groups have a characteristic absorption around 1710 cm<sup>-1</sup>, the signal corresponding to fatty acids and amino acid side chain absorptions. As previously observed by Jiang and Ojeda [12, 49], this IR band showed a small decrease in intensity when the sample pH was increased. Likewise, a band at ~1395 cm<sup>-1</sup>, attributed to the symmetric stretching vibration of carboxylate groups, also showed a dependence on pH (Figure 3.2), in this case increasing in intensity with increasing pH, as expected. In bacterial cell surfaces, phosphate groups can exist in several different forms: inorganic forms of phosphate such as orthophosphate and its oligomers, and organic species in the form of phosphomono- and di-esters. On the basis of the spectral variations reported for different types of phosphates [12], the absorption band at ~ 1227 cm<sup>-1</sup> was assigned to the stretching of the P=O bonds of phosphate diester or protonated polyphosphate. The relative intensity of this band was observed to decrease with increasing solution pH for both *E. coli* and *Y. enterocolitica*, which is consistent with the trends reported for

organophosphates. Another peak corresponding to the stretching of P=O groups of phosphorylated proteins, polyphosphate products, and nucleic acid phosphodiester is observed at  $\sim 1084 \text{ cm}^{-1}$  for both cell types (Figure 3.2). Phosphoryl groups are known to be bound to lipopolysaccharides (LPS), lipids, and muramic acid in the peptidoglycan found in bacterial cell walls [20, 30, 51, 52]. The experiments (Figure 3.2) support the presence of such groups in both bacterial surfaces and suggest that these groups contribute to the overall proton exchange reactivity observed in the titration experiments.

Bacteria FTIR spectra contain prominent features derived from carbohydrate absorption bands, at which C-O-H (alcohol) groups, C-C, and some of the C-O-C vibrations exhibit a broad band in the energy region of  $1200\text{-}950 \text{ cm}^{-1}$  [12, 50, 51]. To compare variations in the occurrence of certain functional groups when cells were grown or acclimatized at different DO levels, the spectrum measured for one treatment was subtracted from the spectrum measured for another treatment. Figure 3.2 shows the difference spectra for both organisms when grown either anaerobically or aerobically and then acclimatized in low DO electrolyte. These spectra reveal that the carbohydrate and phosphoryl bands vary significantly as a function of the growth protocol. For *E. coli* (Figure 3.2a), the phosphoryl or phosphodiester absorption bands exhibit a peak at  $1423 \text{ cm}^{-1}$  and the CHO band shows two distinctive peaks at  $1120$  and  $1084 \text{ cm}^{-1}$ , whereas for *Yersinia*, the peaks are at  $1218 \text{ cm}^{-1}$  (phosphoryl or phosphodiester) and  $1081$  and  $1047 \text{ cm}^{-1}$  (CHO region). Marcotte et al found a strong correlation between the IR-absorption ratio  $A_{\text{sugars}}/A_{\text{amide-II}}$  and variations in polysaccharide content as compared against a leading colorimetric assay [50]. A significant increase in absorption in this area ( $950\text{-}1200 \text{ cm}^{-1}$ ) may be an indication of an increased expression of LPS during anaerobic

growth, as Landini and Zehnder [32] observed with *E. coli* K12 under anoxic growth conditions.

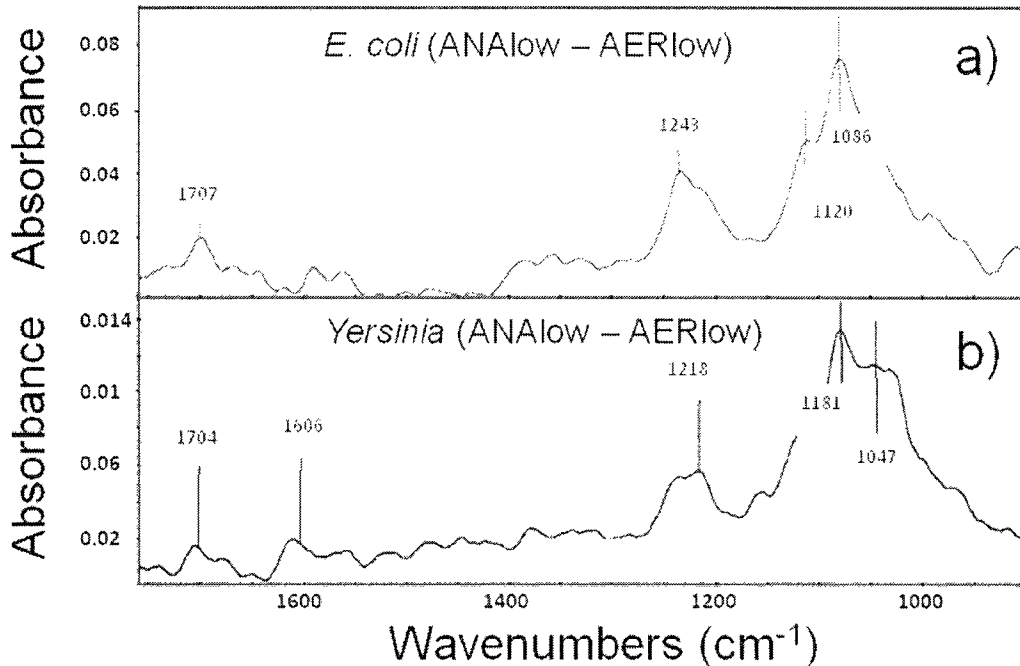


**FIGURE 3.2 :** *E. coli* (a) and *Yersinia* (b) spectra (bottom curves) obtained by difference spectra analysis between aerobic and anaerobic growth for cells acclimatized under low DO at pH 6.7. Differences can be seen at the phosphate and polysaccharide (950-1200 cm<sup>-1</sup>) bands. For further reference see Table 3.3.

The integrated intensity between 950 and 1200 cm<sup>-1</sup> corresponding to the polysaccharide (CHO) absorption region for each of the four treatments is plotted in Figure 3.3 for both organisms. Because all the spectra have been normalized to unit height of the protein amide I band, this integrated intensity is a measure of the CHO:protein ratio. The data for *E. coli* clearly illustrate a larger integrated area (and hence a higher CHO:protein ratio) for the ANA growth treatments in comparison to the AER growth conditions. As discussed above, the higher CHO:protein ratio detected for

anaerobic growth may be linked to increased production of LPS when cells are grown under oxygen depleted conditions. The measurements for *E. coli* also show that the acclimatization treatment (either lowDO or satDO) does not strongly influence the CHO:protein ratio. In contrast, the data obtained from potentiometric titrations and  $\zeta$ -potential (Figure 3.1) indicate that the DO level during cell acclimatization does influence cell surface charge when cells are grown aerobically.

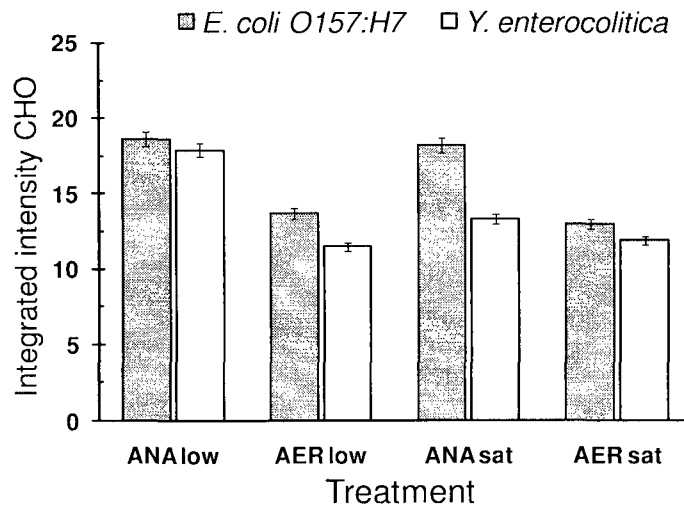


**FIGURE 3.3:** Integrated intensity of carbohydrate IR ( $950\text{-}1200\text{ cm}^{-1}$ ) band for both bacteria suspended in KCl 10 mM at pH 6.7. The bands have been normalized to the amide II band. Bars include 95% confidence interval.

The CHO:protein ratios determined for *Y. enterocolitica* suggest that the ANA low condition presents a unique physicochemical profile in comparison to the three other treatments examined. It is interesting to note that this is in general qualitative agreement with the adhesion behavior of this organism previously reported in Figure 2.1 of Chapter 2 whereby the transport and retention behavior of this organism for the ANA low treatment could not be explained by DLVO theory. The data presented in Figure 3.3 may

suggest increased production of LPS for *Yersinia* cells grown anaerobically and acclimatized in lowDO electrolyte. Such an increase in LPS could explain the enhanced attachment observed in laboratory sand column experiments with the same organism. In previous studies, increased attachment of LPS expressing cells also could not be explained by the DLVO theory of colloidal stability.

The greater polysaccharide/phosphate content detected for *E. coli* grown anaerobically (Figure 3.3) is in qualitative agreement with the increased surface potential and  $S_t$  shown to occur upon switching from aerobic to anaerobic growth, suggesting a probable increase of LPS molecules as also reported in previous studies [35]. In contrast, for *Yersinia*, an increase in the integrated intensity of the CHO band (Figure 3.3) is generally associated with the treatments where lower values of  $S_{tot}$  and  $\zeta$ -potential were observed (Figure 3.1).

### 3.5 Environmental Implications

Complementary studies of potentiometric titration and electrophoretic mobility conducted at pH 6.7 demonstrate a correlation between the deprotonated cell surface functional groups and bacteria  $\zeta$ -potential for both *E. coli* O157:H7 and *Yersinia enterocolitica* (Figure 3.1). For each organism, the amount of deprotonated groups at pH 6.7 agrees very well with the trends observed in the  $\zeta$ -potential measurements. However, when comparing the data for the two organisms, a considerable difference in the magnitude of the  $\zeta$ -potential between the two species is observed, which is not reflected in the calculated amount of deprotonated groups (i.e., the amount of deprotonated groups is quite similar for the two organisms). The very nature of the LPS molecules may play an important role in defining the measured physicochemical properties of the bacteria [18,

25, 35]. The size and structure of the LPS could ultimately determine the outer bacteria electrostatic potential profile. The length, position, and distribution of functional groups, along with their density, can mask or expose charged functional groups that give rise to the measured EPM and hence, the calculated  $\zeta$ -potential. Because LPS can play an important role in cell adhesion to biotic and abiotic surfaces [17, 18, 22, 25, 35, 53], and variations in growth conditions can affect LPS expression in some organisms [18, 25, 32], it is of particular interest to be able to readily characterize the LPS composition of different bacteria over a broad range of environmentally relevant conditions. ATR-FTIR measurements provide a rapid and reliable approach to quantify variations in cell surface composition. However, further studies are needed to study the effect of varying physicochemical conditions on membrane fluidity, protein conformation and LPS content, composition and charge. Finally, the results presented here highlight the dynamic nature of the bacterial cell surface; namely, we observe important differences in cell surface properties over relatively short time scales.

### 3.6 Literature Cited

1. Bradford, S.A., Simunek, J., Walker, S.L, *Transport and straining of E. coli O157:H7 in saturated porous media*. Water Resources Research, 2006. **42**: p. W12S12.
2. Gannon, J.T., V.B. Manilal, and M. Alexander, *Relationship between Cell Surface Properties and Transport of Bacteria through Soil*. Appl. Environ. Microbiol., 1991. **57**(1): p. 190-193.
3. M. Elimelech, J.G., X. Jia, R. A. Williams, *Particle Deposition & Aggregation: Measurement, Modeling and Simulation* ed. Butterworth-Heinemann. 1995.
4. Daughney, C.J., J.B. Fein, and N. Yee, *A comparison of the thermodynamics of metal adsorption onto two common bacteria*. Chemical Geology, 1998. **144**(3-4): p. 161
5. Daughney, C.J., D.A. Fowle, and D. Fortin, *The effect of growth phase on proton and metal adsorption by Bacillus subtilis*. Geochimica et Cosmochimica Acta, 2001. **65**(7): p. 1025-1035.
6. Lalonde, S.V., et al., *Acid-base properties of cyanobacterial surfaces I: Influences of growth phase and nitrogen metabolism on cell surface reactivity*. Geochimica et Cosmochimica Acta, 2008. **72**(5): p. 1257-1268.
7. Haas, J.R., *Effects of cultivation conditions on acid-base titration properties of Shewanella putrefaciens*. Chemical Geology, 2004. **209**(1-2): p. 67-81.
8. Borrok, D.T., B. F.; Fein, J. B. , *A universal surface complexation framework for modeling proton binding onto bacterial surfaces in geologic setting*. Amer. J. Sci. , 2005. **305**: p. 826-853.
9. Borrok, D., et al., *The effect of acidic solutions and growth conditions on the adsorptive properties of bacterial surfaces*. Chemical Geology, 2004. **209**(1-2): p. 107-119.
10. Hong, Y.B., D. G. , *Cell surface acid-base properties of Escherichia coli and Bacillus brevis and variation as a function of growth phase, nitrogen source and C:N ratio*. Coll. Surf. B, 2006. **50**: p. 112-119.
11. Eboigbodin, K.E., J.J. Ojeda, and C.A. Biggs, *Investigating the Surface Properties of Escherichia coli under Glucose Controlled Conditions and Its Effect on Aggregation*. Langmuir, 2007. **23**(12): p. 6691-6697.

12. Jiang, W., et al., Elucidation of Functional Groups on Gram-Positive and Gram-Negative Bacterial Surfaces Using Infrared Spectroscopy. *Langmuir*, 2004. **20**(26): p. 11433-11442.
13. Castro, F.D. and N. Tufenkji, Relevance of Nontoxigenic Strains as Surrogates for *Escherichia coli* O157:H7 in Groundwater Contamination Potential: Role of Temperature and Cell Acclimation Time. *Environ. Sci. Technol.*, 2007. **41**(12): p. 4332-4338.
14. Yang, H.H., et al., Intestinal versus External Growth Conditions Change the Surficial Properties in a Collection of Environmental *Escherichia coli* Isolates. *Environ. Sci. Technol.*, 2006. **40**(22): p. 6976-6982.
15. Harvey, R., Harms, H., Transport of Microorganisms in the Terrestrial Subsurface: In Situ and Laboratory Methods. *Manual of Environmental Microbiology*, 2001: p. 753-776.
16. Scholl, M.A. and R.W. Harvey, Laboratory investigations on the role of sediment surface and groundwater chemistry in transport of bacteria through a contaminated sandy aquifer. *Environ. Sci. Technol.*, 1992. **26**(7): p. 1410-1417.
17. Beveridge, T.J. and L.L. Graham, *Surface layers of bacteria*. *Microbiol. Mol. Biol. Rev.*, 1991. **55**(4): p. 684-705.
18. Korenevsky, A. and T.J. Beveridge, The surface physicochemistry and adhesiveness of *Shewanella* are affected by their surface polysaccharides. *Microbiology*, 2007. **153**(6): p. 1872-1883.
19. Fein, J.B., et al., Potentiometric titrations of *Bacillus subtilis* cells to low pH and a comparison of modeling approaches. *Geochimica et Cosmochimica Acta*, 2005. **69**(5): p. 1123-1132.
20. Yee, N., et al., Characterization of Metal-Cyanobacteria Sorption Reactions: A Combined Macroscopic and Infrared Spectroscopic Investigation. *Environ. Sci. Technol.*, 2004. **38**(3): p. 775-782.
21. Beveridge, T.J. and R.G. Murray, *Sites of metal deposition in the cell wall of Bacillus subtilis*. *J. Bacteriol.*, 1980. **141**(2): p. 876-887.
22. Walker, S.L., J.A. Redman, and M. Elimelech, Role of Cell Surface Lipopolysaccharides in *Escherichia coli* K12 Adhesion and Transport. *Langmuir*, 2004. **20**(18): p. 7736-7746.

23. Cox, A.D. and S.G. Wilkinson, Ionizing groups in lipopolysaccharides of *Pseudomonas cepacia* in relation to antibiotic resistance. *Molecular Microbiology*, 1991. **5**(3): p. 641-646.
24. Martinez, R.E., et al., Determination of Intrinsic Bacterial Surface Acidity Constants using a Donnan Shell Model and a Continuous pKa Distribution Method. *Journal of Colloid and Interface Science*, 2002. **253**(1): p. 130-139.
25. Phoenix, V., et al., Influence of Lipopolysaccharide on the Surface Proton-Binding Behavior of *Shewanella* spp. *Current Microbiology*, 2007. **55**(2): p. 152-157.
26. Sokolov, I., et al., Cell Surface Electrochemical Heterogeneity of the Fe(III)-Reducing Bacteria *Shewanella putrefaciens*. *Environ. Sci. Technol.*, 2001. **35**(2): p. 341-347.
27. Naumann, D., FT-Infrared and FT-Raman Spectroscopy in Biomedical Research, in *Infrared and Raman spectroscopy of biological materials*, H. Gremlich, Yan, B., Eds., Editor. 2000, Marcel Dekker Inc.: New York. p. p 323.
28. Naumann, D., D. Helm, and H. Labischinski, *Microbiological characterizations by FT-IR spectroscopy*. *Nature*, 1991. **351**(6321): p. 81-82.
29. Parikh, S.J. and J. Chorover, ATR-FTIR Spectroscopy Reveals Bond Formation During Bacterial Adhesion to Iron Oxide. *Langmuir*, 2006. **22**(20): p. 8492-8500.
30. Parikh, S.J. and J. Chorover, *Infrared spectroscopy studies of cation effects on lipopolysaccharides in aqueous solution*. *Colloids and Surfaces B: Biointerfaces*, 2007. **55**(2): p. 241-250.
31. Dittrich, M. and S. Sibling, Cell surface groups of two picocyanobacteria strains studied by zeta potential investigations, potentiometric titration, and infrared spectroscopy. *Journal of Colloid and Interface Science*, 2005. **286**(2): p. 487-495.
32. Leone, L., et al., Modeling the Acid-Base Properties of Bacterial Surfaces: A Combined Spectroscopic and Potentiometric Study of the Gram-Positive Bacterium *Bacillus subtilis*. *Environ. Sci. Technol.*, 2007. **41**(18): p. 6465-6471.
33. Cox, J.S., et al., Characterizing Heterogeneous Bacterial Surface Functional Groups Using Discrete Affinity Spectra for Proton Binding. *Environ. Sci. Technol.*, 1999. **33**(24): p. 4514-4521.

34. Schmitt, J. and H.-C. Flemming, *FTIR-spectroscopy in microbial and material analysis*. International Biodeterioration & Biodegradation, 1998. **41**(1): p. 1.
35. Landini, P. and A.J.B. Zehnder, The Global Regulatory hns Gene Negatively Affects Adhesion to Solid Surfaces by Anaerobically Grown Escherichia coli by Modulating Expression of Flagellar Genes and Lipopolysaccharide Production. J. Bacteriol., 2002. **184**(6): p. 1522-1529.
36. Yang, H.-H., The Effect of Environmental Stress on Cell Surface Properties and Their Relation to Microbial Adhesion in Feedlot Escherichia coli Isolates. 2005, University of Connecticut.
37. Goldscheider, N., D. Hunkeler, and P. Rossi, *Review: Microbial biocenoses in pristine aquifers and an assessment of investigative methods*. Hydrogeology Journal, 2006. **V14**(6): p. 926.
38. Datry, T., F. Malard, and J. Gibert, Dynamics of solutes and dissolved oxygen in shallow urban groundwater below a stormwater infiltration basin. Science of the Total Environment, 2004. **329**(1-3): p. 215-229.
39. Herbelin, A.L.W., J. C., "FITEQL - A Computer Program for Determination of Chemical Equilibrium Constants from Experimental Data. Report 99-01,". 1999, Department of Chemistry, Oregon State University: Corvallis, OR.
40. Rahmelow, K. and W. Hubner, Infrared Spectroscopy in Aqueous Solution: Difficulties and Accuracy of Water Subtraction. Applied Spectroscopy, 1997. **51**: p. 160-170.
41. Etzion, Y., et al., Determination of Protein Concentration in Raw Milk by Mid-Infrared Fourier Transform Infrared/Attenuated Total Reflectance Spectroscopy. J. Dairy Sci., 2004. **87**(9): p. 2779-2788.
42. Dittrich, M. and S. Sibler, Influence of H<sup>+</sup> and Calcium Ions on Surface Functional Groups of Synechococcus PCC 7942 Cells. Langmuir, 2006. **22**(12): p. 5435-5442.
43. Ngwenya, B.T., I.W. Sutherland, and L. Kennedy, Comparison of the acid-base behaviour and metal adsorption characteristics of a gram-negative bacterium with other strains. Applied Geochemistry, 2003. **18**(4): p. 527-538.

44. Fein, J.B., et al., Potentiometric titrations of *Bacillus subtilis* cells to low pH and a comparison of modeling approaches. *Geochimica et Cosmochimica Acta*, 2005. **69**(5): p. 1123.
45. Fontes, D.E., et al., Physical and chemical factors influencing transport of microorganisms through porous media. *Appl. Environ. Microbiol.*, 1991. **57**(9): p. 2473-2481.
46. Ryan, J.N.E., M., *Colloid mobilization and transport in groundwater*. . Coll. Surf. A, 1996. **107**: p. 1-56.
47. Roberts, J.A., et al., Attachment Behavior of *Shewanella putrefaciens* onto Magnetite under Aerobic and Anaerobic Conditions. *Geomicrobiology Journal*, 2006. **23**(8): p. 631-640.
48. Tourney, J., et al., The effect of extracellular polymers (EPS) on the proton adsorption characteristics of the thermophile *Bacillus licheniformis* S-86. *Chemical Geology*, 2008. **247**(1-2): p. 1-15.
49. Ojeda, J.J., et al., Characterization of the Cell Surface and Cell Wall Chemistry of Drinking Water Bacteria by Combining XPS, FTIR Spectroscopy, Modeling, and Potentiometric Titrations. *Langmuir*, 2008. **24**(8): p. 4032-4040.
50. Marcotte, L., et al., An alternative infrared spectroscopy assay for the quantification of polysaccharides in bacterial samples. *Analytical Biochemistry*, 2007. **361**(1): p. 7-14.
51. Parikh, S.J. and J. Chorover, *ATR-FTIR study of lipopolysaccharides at mineral surfaces*. *Colloids and Surfaces B: Biointerfaces*, 2008. **62**(2): p. 188-198.
52. Stenutz, R., A. Weintraub, and G. Widmalm, *The structures of Escherichia coli O-polysaccharide antigens*. *FEMS Microbiology Reviews*, 2006. **30**(3): p. 382-403.
53. Hermansson, M., *The DLVO theory in microbial adhesion*. *Colloids and Surfaces B: Biointerfaces*, 1999. **14**(1-4): p. 105-119.
54. Grasso, D., et al., *A review of non-DLVO interactions in environmental colloidal systems*. *Reviews in Environmental Science and Biotechnology*, 2002. **1**(1): p. 17-38.
55. Makin SA, B.T., *Pseudomonas aeruginosa* PAO1 ceases to express serotype-specific lipopolysaccharide at 45C. *J Bacteriol*, 1996. **178**: p. 3350-3352.

## CHAPTER 4

### Conclusions

Well-controlled laboratory-scale column deposition experiments in clean quartz sand of two selected bacterial pathogens at 11°C and pH 6.7 provided evidence of the direct effect of extreme dissolved oxygen (DO) concentrations during growth (anaerobic and aerobic) and acclimation for 21h (microaerophilic and saturated) on bacterial retention in granular porous media. Results suggest that lack of oxygen during growth and acclimation is an environmental signal that reduces cell adhesion of *E. coli*. For this bacterium, attachment efficiencies agree in all cases with the classic DLVO framework considering surface charge potential electrostatic repulsion estimated by EPM or zeta potential. On the contrary, *Yersinia* adhesion to sand was negatively influenced by high oxygen concentrations during growth and acclimation. In general adhesion correlated with DLVO however greater adhesion was observed under anaerobic growth and low DO acclimation that could not be explained only by electrostatic repulsion. A microscopic approach allowed to identify major functional groups associated with the bacteria surface charge and their corresponding variations with the treatments studied. A possible role of the LPS revealed by FTIR spectra analysis and titration of cells, was hypothesized due to its known role on initial cell-surface interactions is related to the formation of hydrogen bonds between bacterial cells and the solid surface and its chemical composition, chain length, and overall charge of the LPS determine the nature of cell-surface interaction, allowing either attraction or repulsion forces to prevail.

## APPENDIX

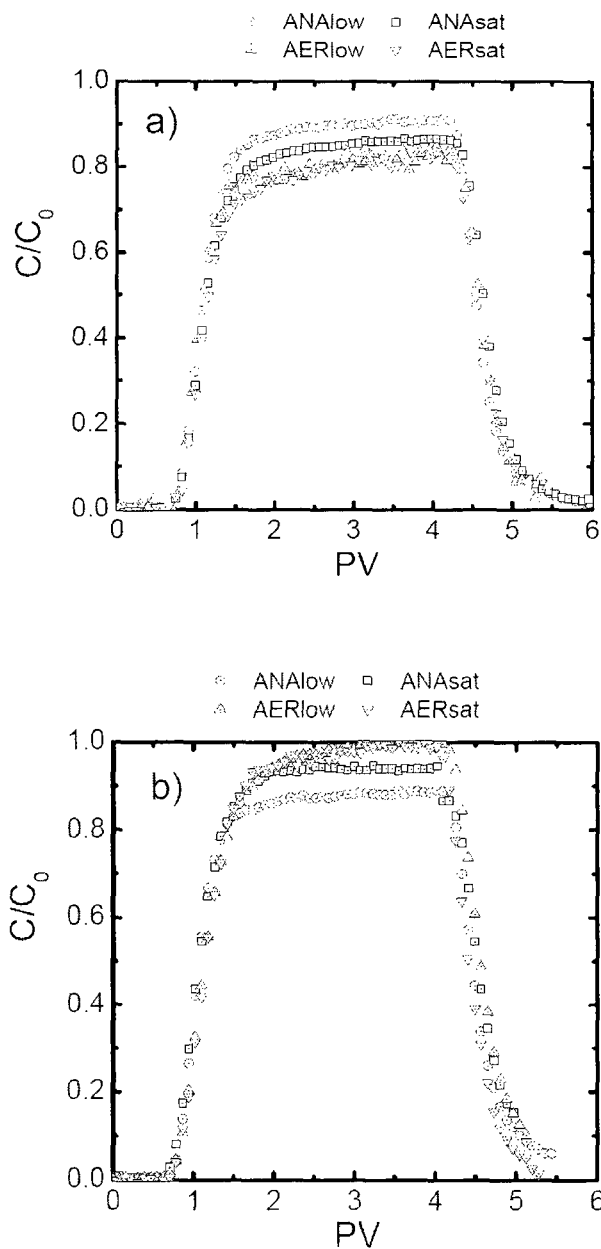


**FIGURE 1:** Representative bacteria breakthrough curves of the four treatments considered. a) *E. coli* O157:H7 and b) *Yersinia enterocolitica*. Column experiments were conducted at 11 °C and pH 6.7. PV is the pore volume;  $C/C_0$  is the normalized bacteria concentration.